Electronic Supplementary Material (ESI) for New Journal of Chemistry.

Electronic Supplementary Information

Synthesis of a Half-Sandwich Complex of Ruthenium(II) with a Nonsymmetric Bis-Nitrogen Donor Ligand: Biological Investigations

Sana Yarahmadi,[a] Elham Jokar,[b,c] Zahra Shamsi,[a] Dalia Nahieh,[b,c] Mehrnoosh Moosavi,[b] Masood Fereidoonnezhad,[b,c] and Hamid R. Shahsavari[a*]*

[a]Department of Chemistry, Institute for Advanced Studies in Basic Sciences (IASBS), Zanjan 45137-66731, Iran. *E-mail: shahsavari@iasbs.ac.ir.

[b]Toxicology Research Center, Medical Basic Sciences Research Institute, Ahvaz Jundishapur University of Medical Sciences, Ahvaz, Iran.

[c]Department of Medicinal Chemistry, Faculty of Pharmacy, Ahvaz Jundishapur University of Medical Sciences, Ahvaz, Iran. *E-mail: fereidoonnezhad-m@ajums.ac.ir.

Contents:	**Page**

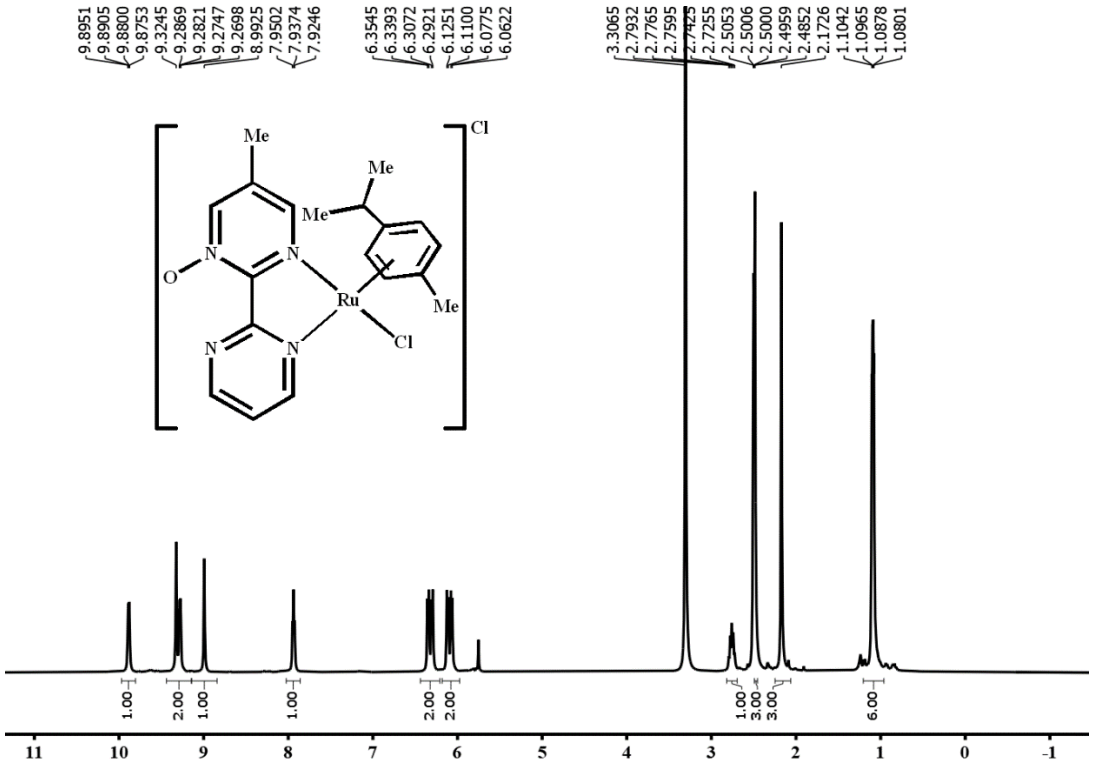

Figure S1. ^{1}H NMR spectrum of **1** in dmso-*d*$_6$.

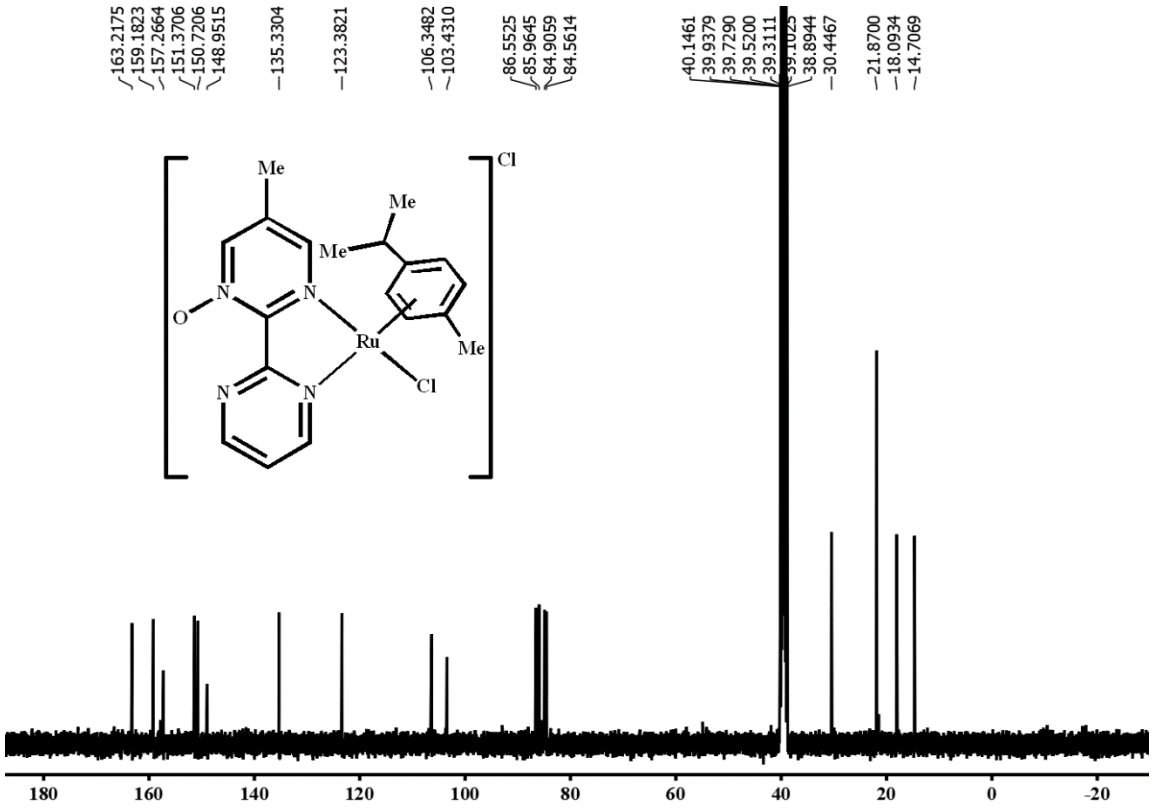

Figure S2. ^{13}C{^{1}H} NMR spectrum of **1** in dmso-*d*$_6$.

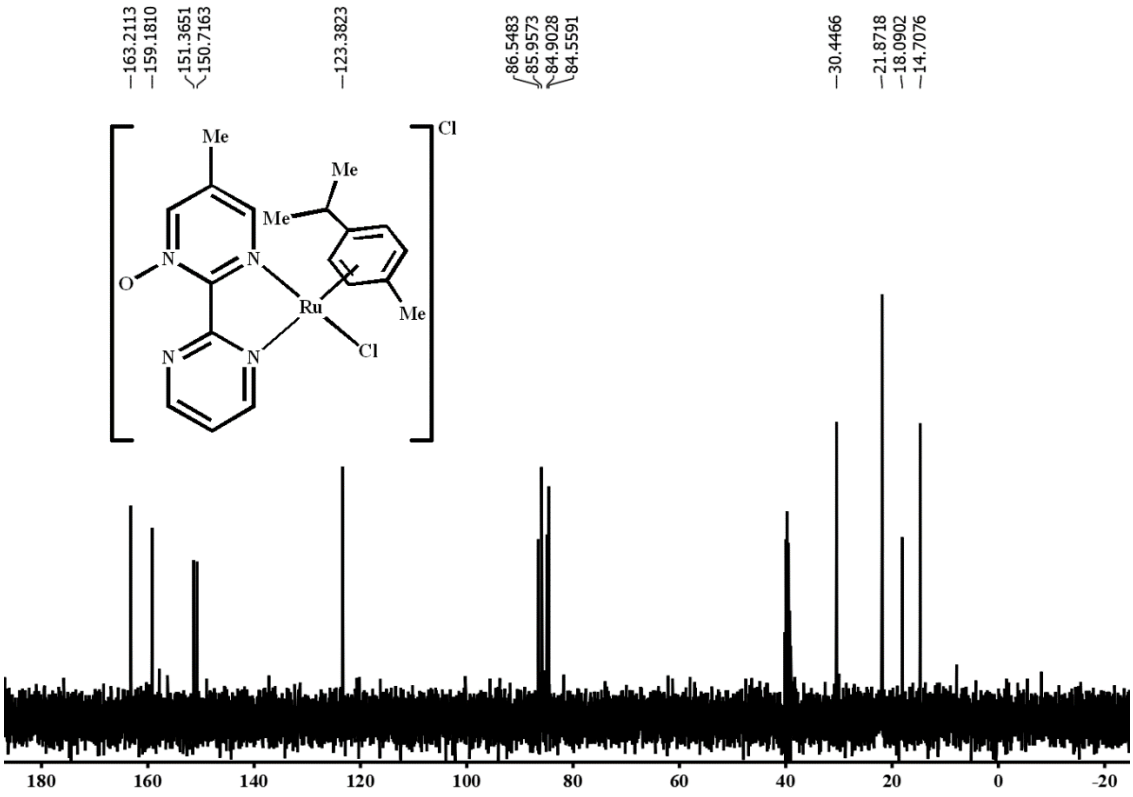

Figure S3. DEPT-135° spectrum of **1** in dmso-d_6.

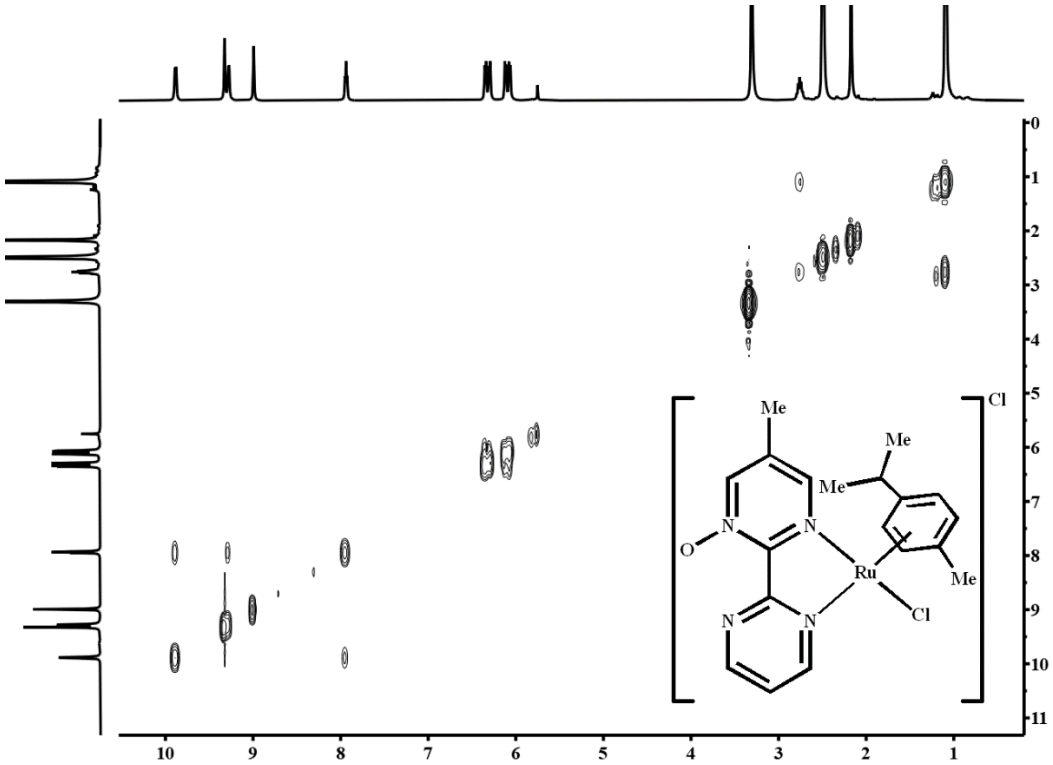

Figure S4. $^{1}H^{1}H$COSY spectrum of **1** in dmso-d_6.

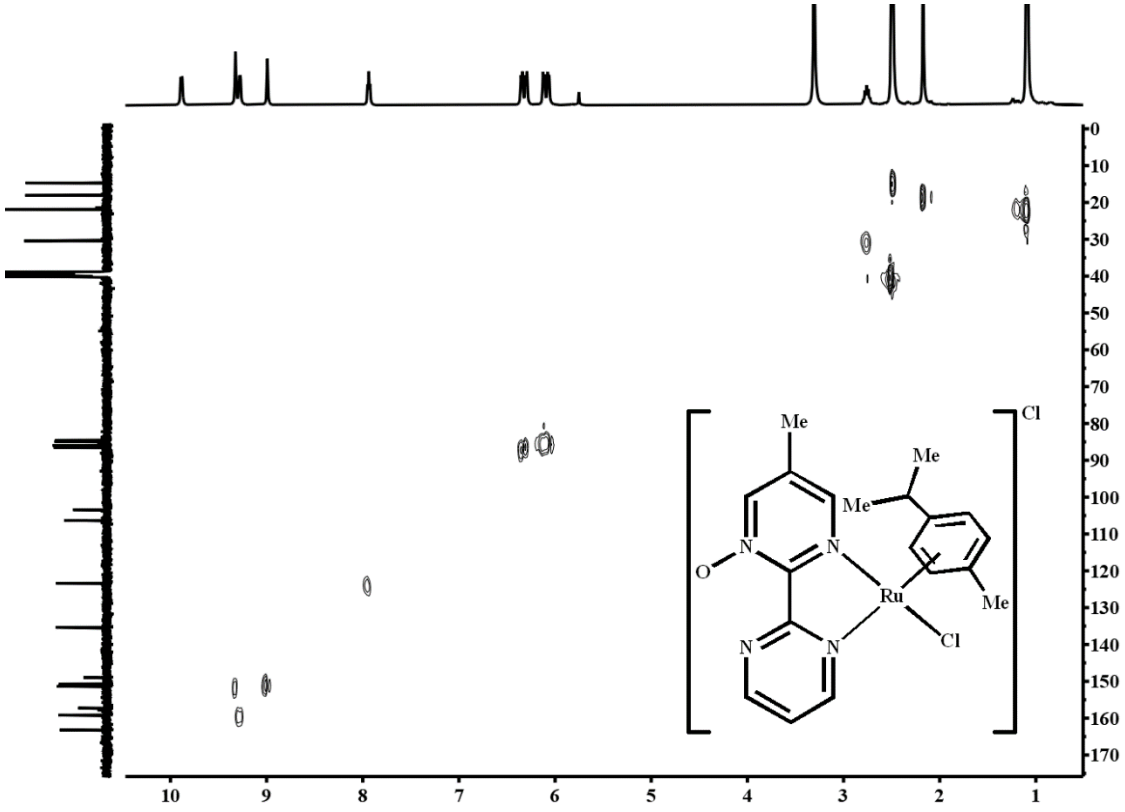

Figure S5. HSQC spectrum of **1** in dmso-d_6.

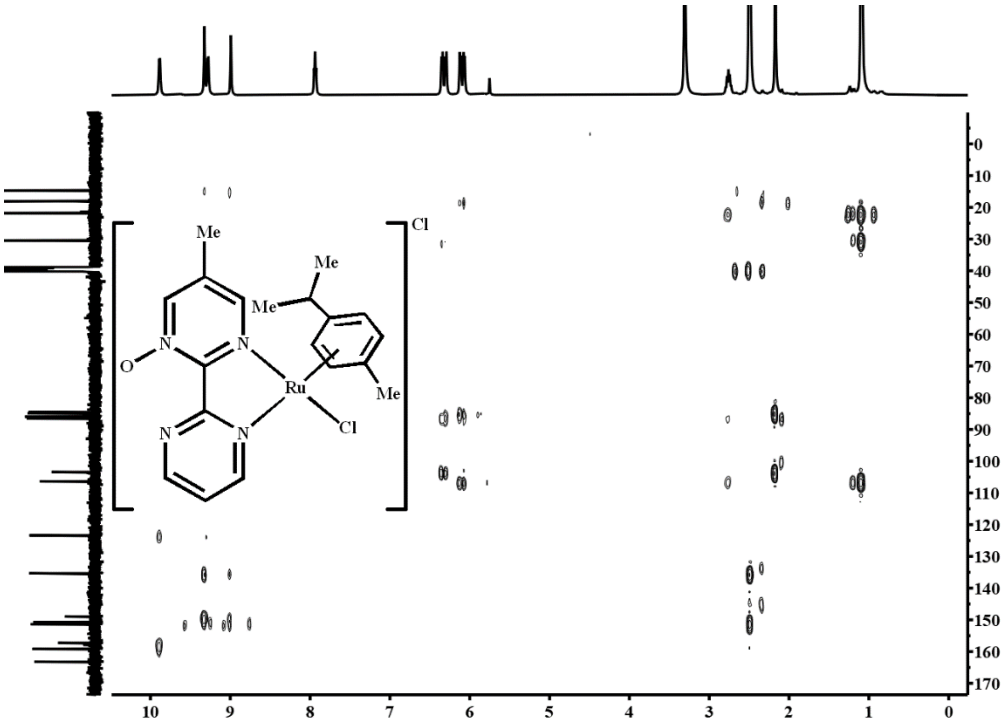

Figure S6. HMBC spectrum of **1** in dmso-d_6.

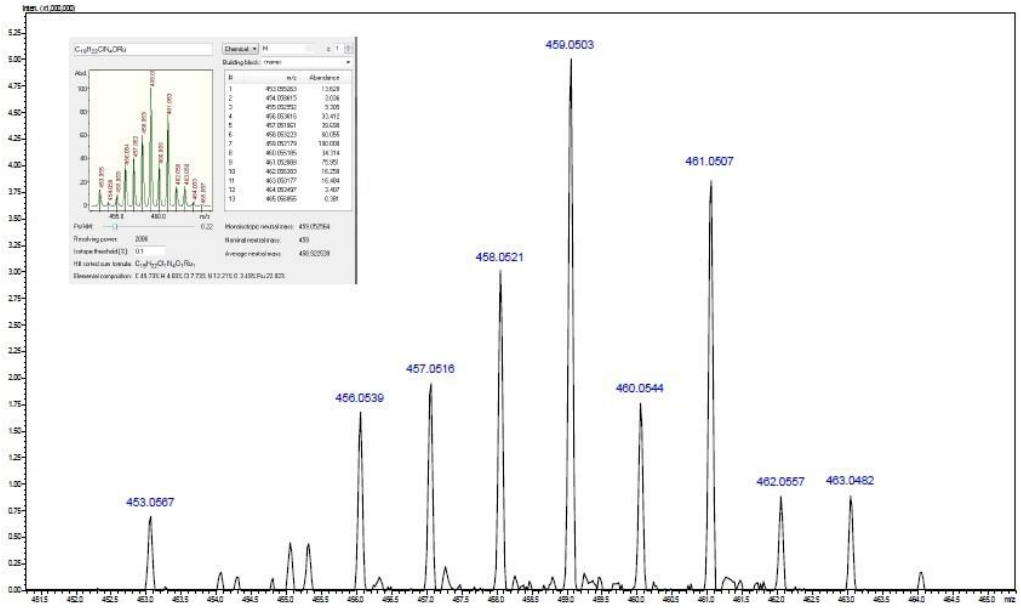

Figure S7. HR ESI-Mass spectrum of **1**. Inset shows the calculated pattern.

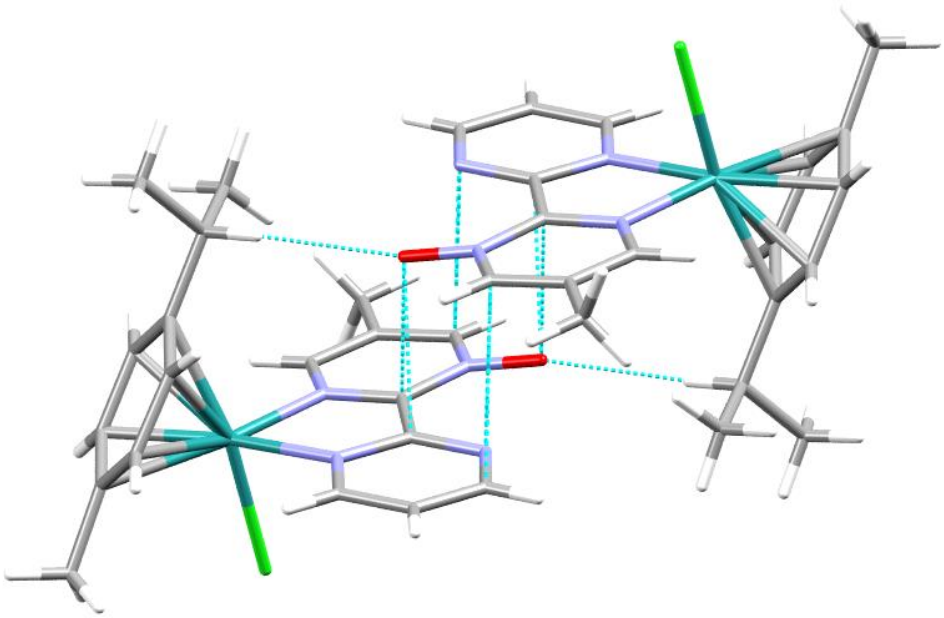

Figure S8. Partial view of crystal packing of **1**.

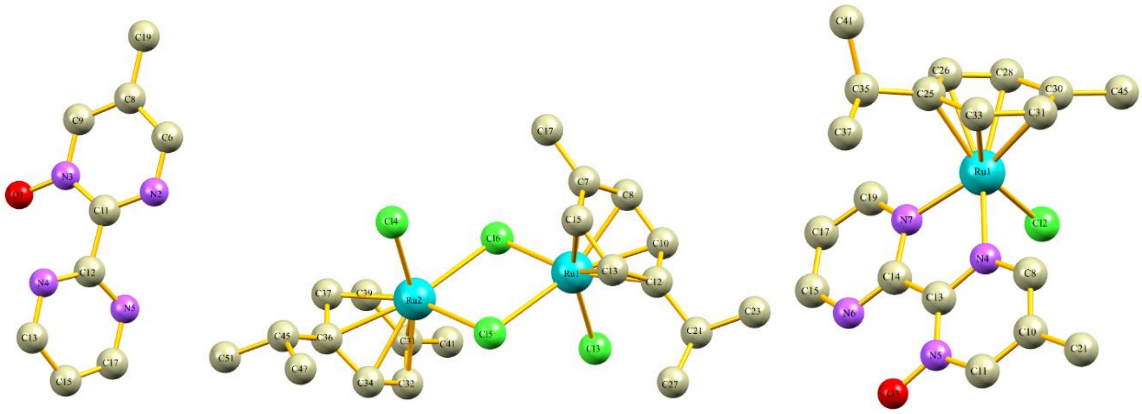

Figure S9. View of the optimized structures of **A** (middle), **B** (left), and **1** (right) in dmso with the atom numbering (the chloride counter anion is omitted in **1** for clarity).

Table S1. Selected bond distances (A°) and angles (deg) for the calculated (S_0 in gas phase and in dmso) of **A**.

Bond distance or angle	Crystal Structure	S_0 (gas phase)	S_0 (dmso)
Ru(1)-Cl(3)	2.416(3)	2.434	2.469
Ru(1)-Cl(5)	2.451	2.504	2.530
Ru(1)-Cl(6)	2.464	2.504	2.531
Ru(1)-Ring(Centroid)	1.658	1.719	1.738
Cl(3)-Ru(1)-Cl(6)	85.22	87.89	87.53
Cl(5)-Ru(1)-Cl(6)	82.53	82.77	82.00
Cl(3)-Ru(1)-Cl(5)	87.18	88.01	87.53
Cl(5)-Ru(1)-Ring(Centroid)	127.98	127.24	128.86
Cl(6)-Ru(1)-Ring(Centroid)	128.82	127.54	128.70
Cl(3)-Ru(1)-Ring(Centroid)	128.88	128.70	127.60

Table S2. Selected bond distances (A°) and angles (deg) for the calculated (S_0 in gas phase and in dmso) of **1**.

Bond distance or angle	Crystal Structure	S_0 (gas phase)	S_0 (dmso)
Ru(1)-Cl(1)	2.401(7)	2.4132	2.4584
Ru(1)-N(1)	2.097(2)	2.1140	2.1128
Ru(1)-N(4)	2.077(2)	2.0875	2.0899
Ru(1)-Ring(Centroid)	1.683	1.812	1.813
N(1)-Ru(1)-N(4)	77.07(8)	76.99	76.78
Cl(1)-Ru(1)-N(1)	82.76(6)	84.77	85.48
Cl(1)-Ru(1)-N(4)	84.49(6)	84.19	85.15
Cl(1)-Ru(1)-Ring(Centroid)	129.16	125.57	126.55
N(1)-Ru(1)-Ring(Centroid)	133.39	133.32	132.22
N(4)-Ru(1)-Ring(Centroid)	130.84	133.58	133.66

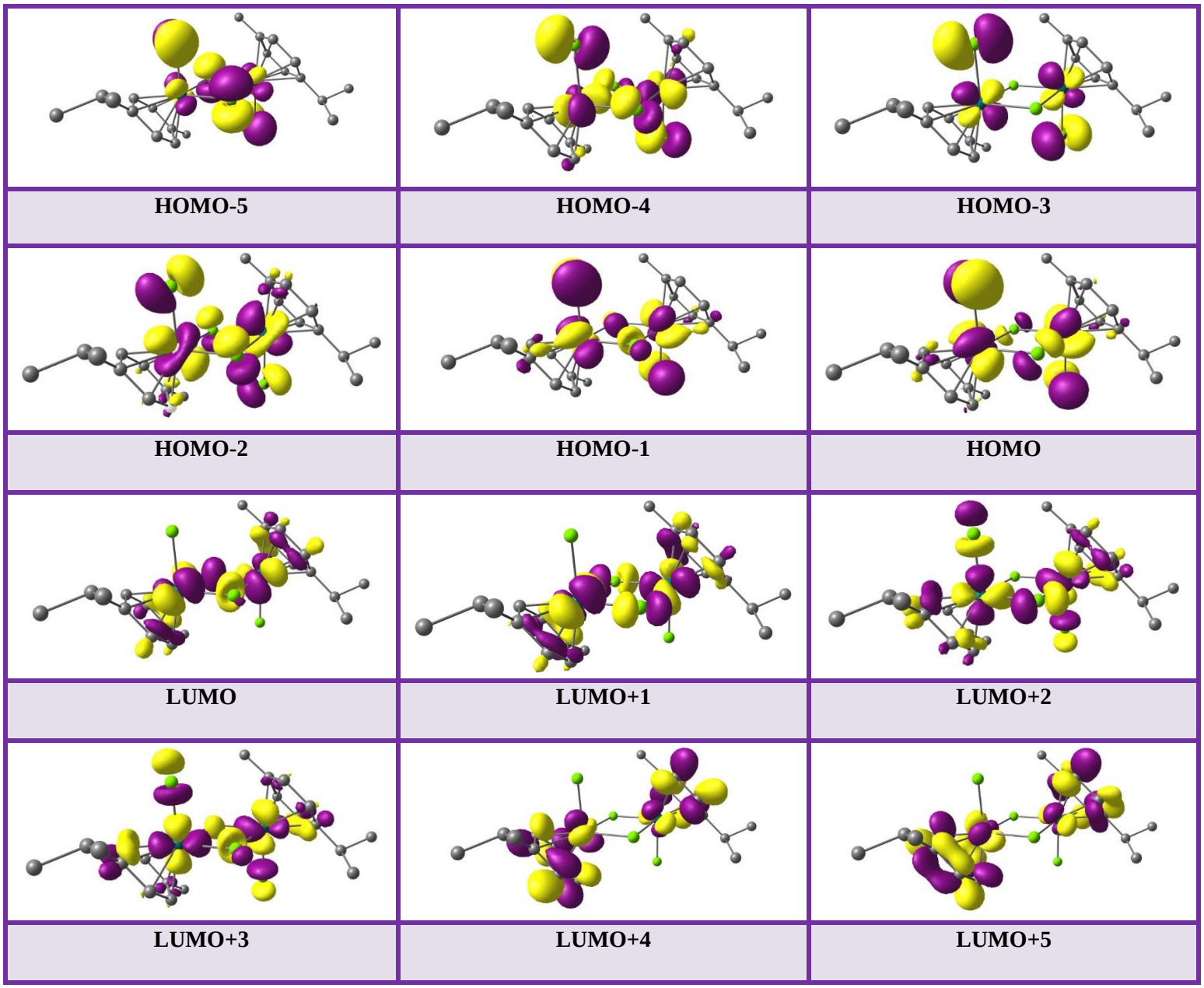

Figure S10. Molecular orbital plots for the optimized structure of **A** in gas phase.

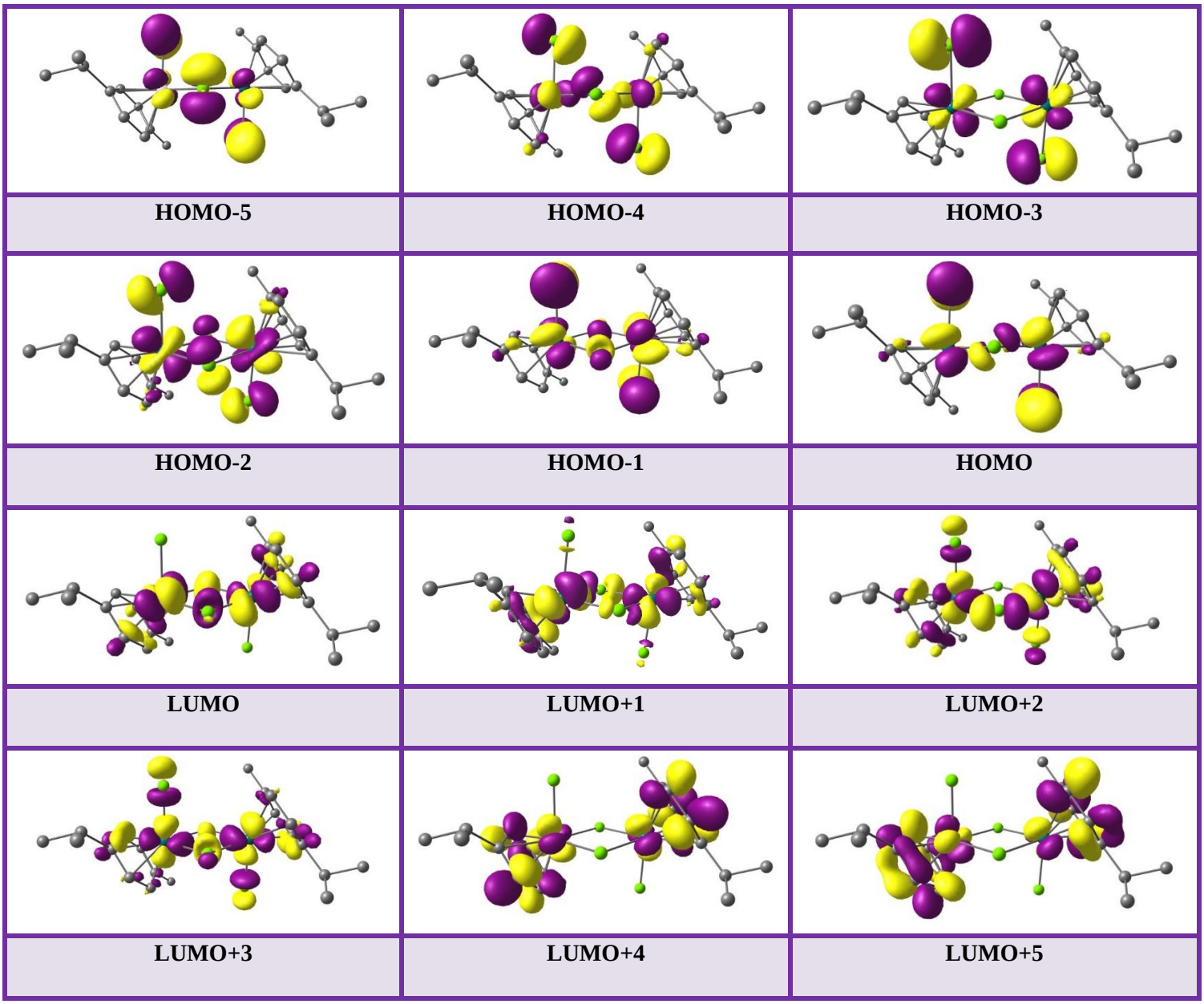

Figure S11. Molecular orbital plots for the optimized structure of **A** in dmso solution.

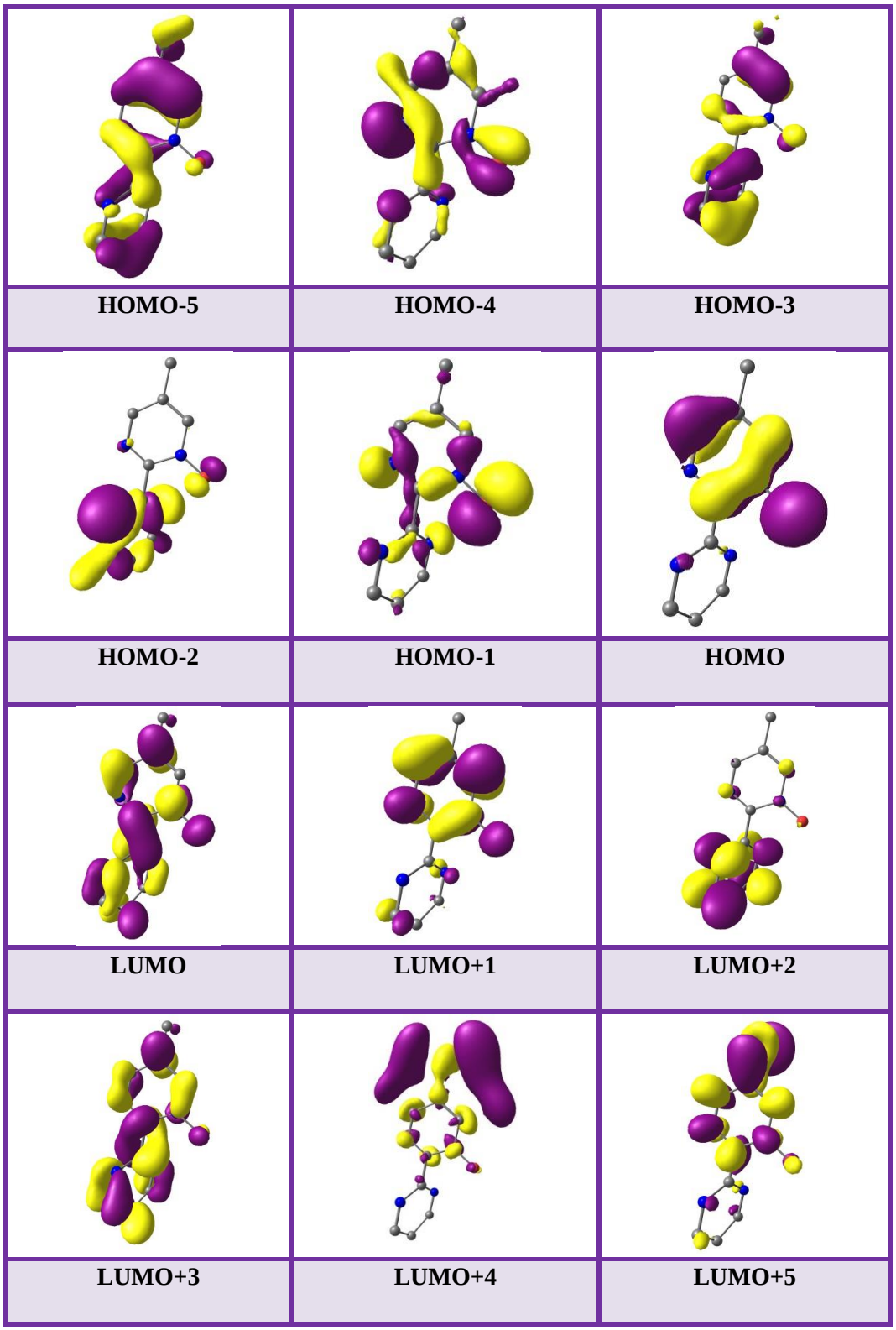

Figure S12. Molecular orbital plots for the optimized structure of **B** in gas phase.

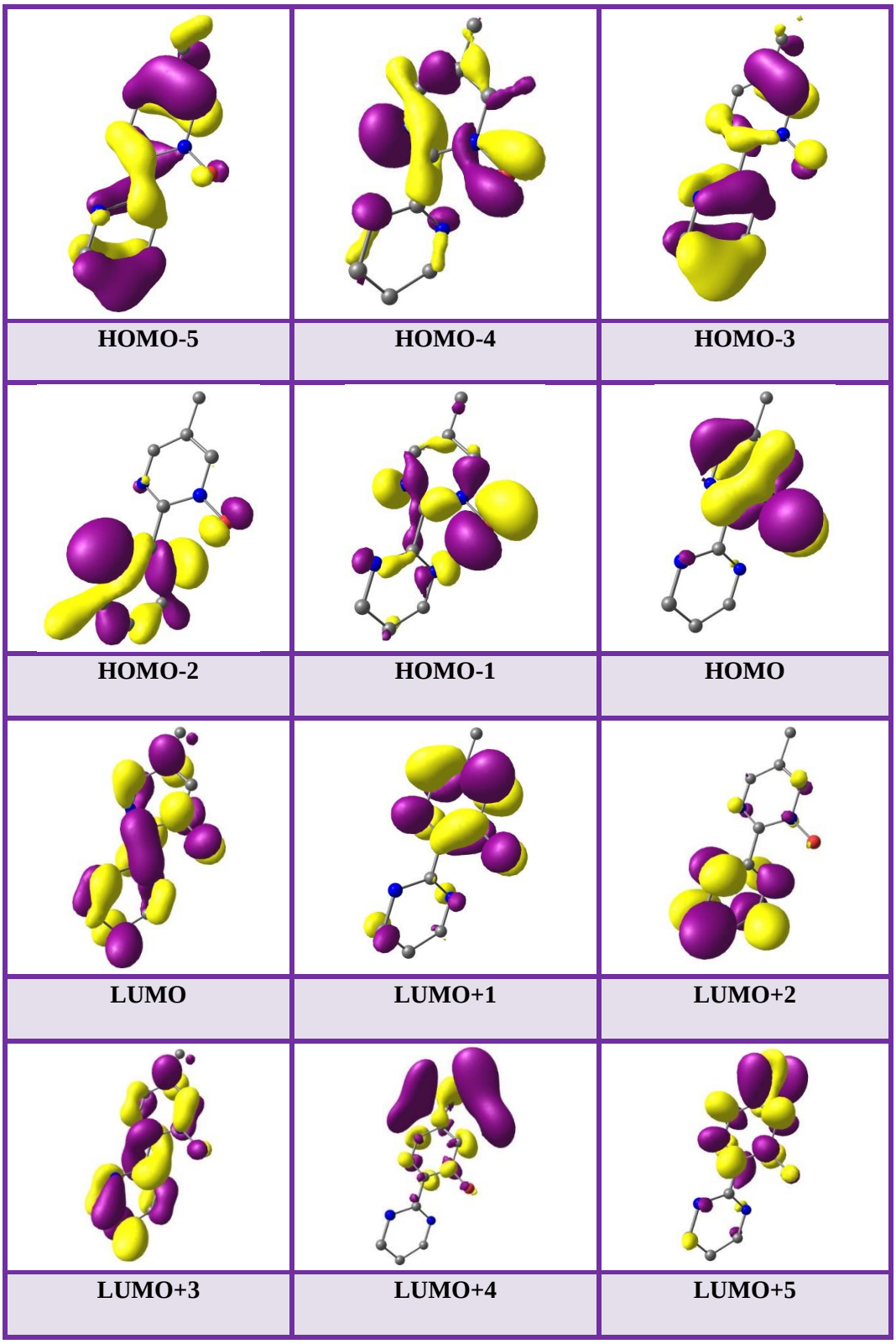

Figure S13. Molecular orbital plots for the optimized structure of **B** in dmso solution.

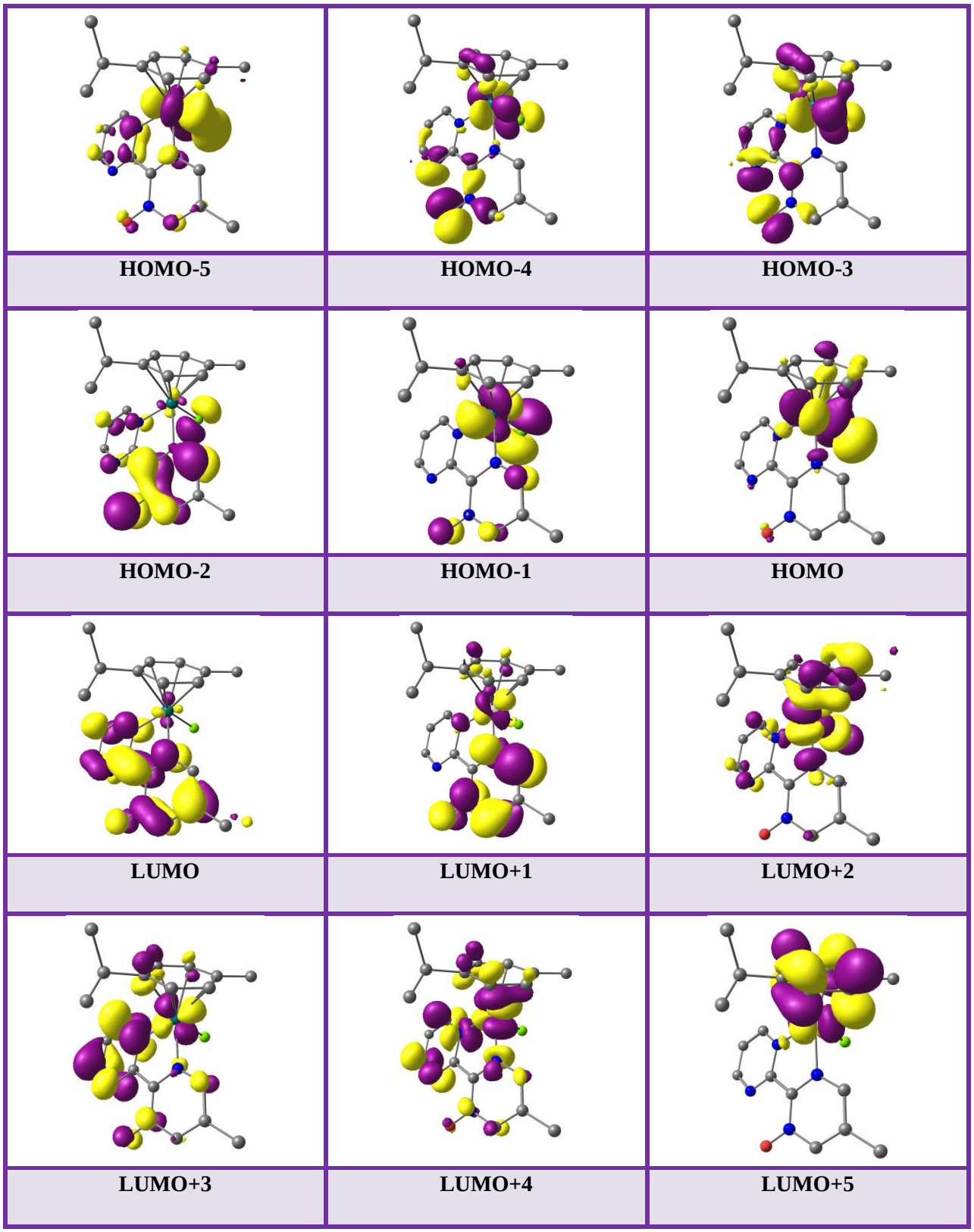

Figure S14. Molecular orbital plots for the optimized structure of **1** in gas phase.

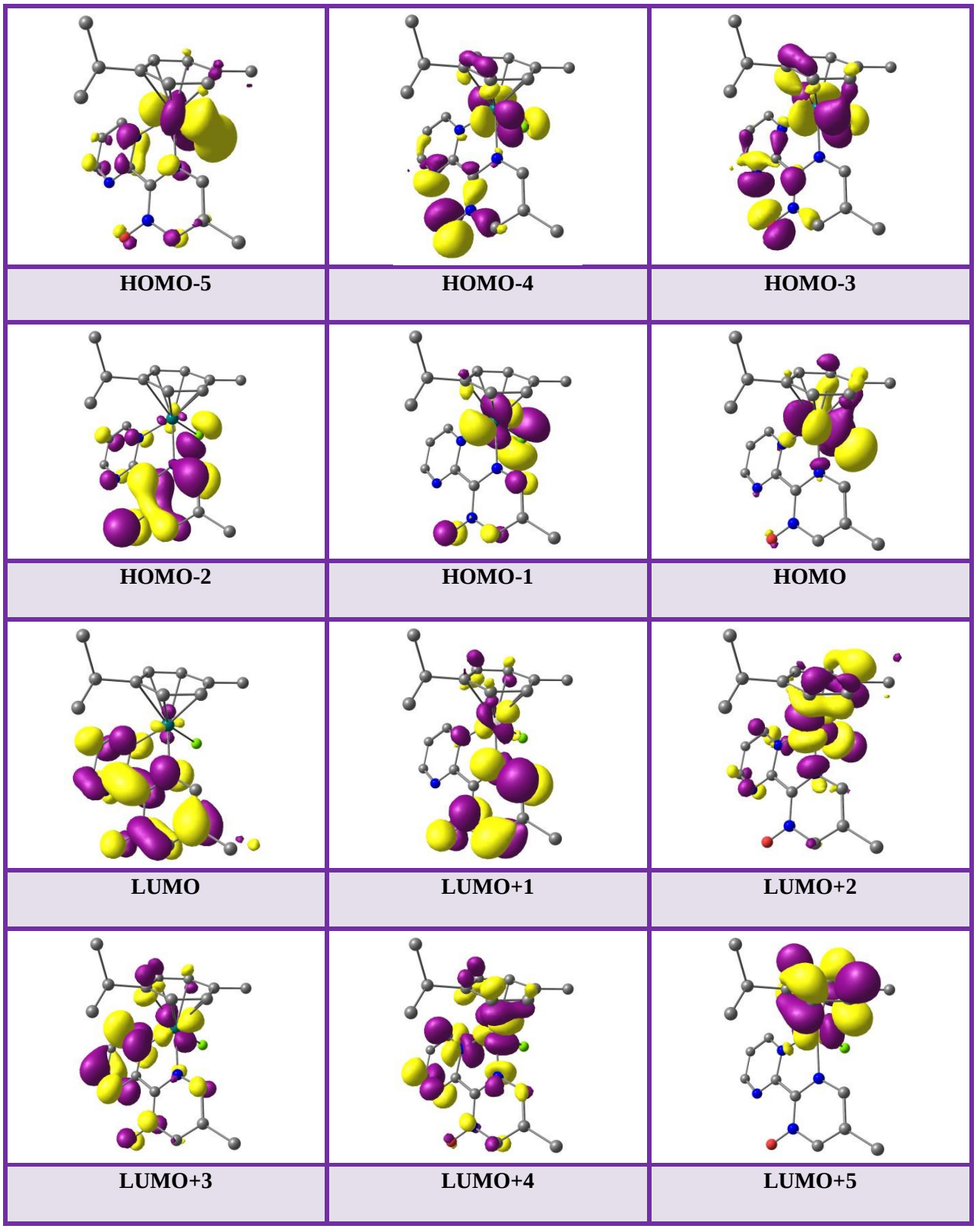

Figure S15. Molecular orbital plots for the optimized structure of **2** in dmso solution.

Table S3. The energies of the selected molecular orbitals of **A** with their compositions in gas phase.

A							
	Energy	Components(%)					
MO	(eV)	Ru_1	L_1=*p*-cymene$_{(7\text{-}30)}$	L_2=Cl_3	L_3=Cl_5	L_4=Cl_6	Other
LUMO+5	-0.548	10	39	0	0	1	50
LUMO+4	-0.553	9	41	1	0	0	49
LUMO+3	-1.575	26	11	7	7	4	45
LUMO+2	-1.684	27	12	7	6	2	46
LUMO+1	-1.809	29	13	1	4	11	42
LUMO	-2.070	28	11	1	9	11	40
HOMO	-5.638	19	8	18	6	4	45
HOMO-1	-5.714	17	9	19	5	5	45
HOMO-2	-5.771	23	9	12	7	7	42
HOMO-3	-5.989	17	5	27	1	0	50
HOMO-4	-6.049	18	7	18	7	8	42
HOMO-5	-6.526	6	3	18	24	22	27

Table S4. The energies of the selected molecular orbitals of **A** with their compositions in dmso solution.

A							
	Energy	Components(%)					
MO	(eV)	Ru_1	L_1=*p*-cymene$_{(7\text{-}30)}$	L_2=Cl_3	L_3=Cl_5	L_4=Cl_6	Other
LUMO+5	-0.551	10	40	0	0	1	49
LUMO+4	-0.584	9	40	1	0	0	50
LUMO+3	-1.669	27	11	7	6	3	46
LUMO+2	-1.759	28	12	6	9	0	45
LUMO+1	-1.878	28	12	2	3	12	43
LUMO	-2.167	29	10	1	9	11	40
HOMO	-5.606	18	8	19	5	4	46
HOMO-1	-5.693	16	8	21	5	5	45
HOMO-2	-5.730	22	8	13	7	6	44
HOMO-3	-5.944	17	4	29	0	0	50
HOMO-4	-6.045	12	7	23	9	8	41
HOMO-5	-6.444	8	3	15	24	23	27

Table S5. The energies of the selected molecular orbitals of **B** with their compositions in dmso solution.

B									
	Energy	Components(%)							
MO	(eV)	O	N_2	N_3	N_4	N_5	Me	$Ring_{6-11}$	$Ring_{12-18}$
LUMO+5	2.762	0	4	3	1	1	67	20	4
LUMO+4	2.506	0	1	1	0	0	60	36	2
LUMO+3	-0.479	1	3	5	4	4	4	34	45
LUMO+2	-1.066	1	2	1	18	21	0	4	53
LUMO+1	-1.303	7	21	14	2	1	3	46	6
LUMO	-1.355	6	3	13	7	6	3	33	29
HOMO	-5.938	52	0	3	1	1	1	40	2
HOMO-1	-6.576	54	12	2	5	2	2	17	6
HOMO-2	-6.898	4	2	0	32	35	0	2	25
HOMO-3	-7.730	3	8	1	5	5	4	27	47
HOMO-4	-7.892	14	44	6	2	2	2	25	5
HOMO-5	-8.114	2	6	1	2	3	6	48	32

Table S6. The energies of the selected molecular orbitals of **1** with their compositions in gas phase.

1					
	Energy	Components(%)			
MO	(eV)	Ru	bpyNO	*p*-cymene	Cl
LUMO+5	-3.943	19	6	73	2
LUMO+4	-4.652	35	50	15	0
LUMO+3	-4.887	22	65	12	1
LUMO+2	-4.966	43	19	24	14
LUMO+1	-5.076	10	79	9	2
LUMO	-5.747	3	92	3	2
HOMO	-9.052	37	7	14	42
HOMO-1	-9.272	39	8	13	40
HOMO-2	-9.581	3	79	1	17
HOMO-3	-9.953	31	47	11	11
HOMO-4	-10.006	18	63	8	11
HOMO-5	-10.520	33	17	8	42

Table S7. The energies of the selected molecular orbitals of **1** with their compositions in dmso solution.

1					
	Energy	Components(%)			
MO	(eV)	Ru	bpyNO	*p*-cymene	Cl
LUMO+5	-1.008	17	5	76	2
LUMO+4	-1.827	41	42	17	0
LUMO+3	-2.091	17	72	10	1
LUMO+2	-2.207	41	28	19	12
LUMO+1	-2.313	15	69	10	6
LUMO	-2.993	4	92	2	2
HOMO	-6.475	50	8	15	27
HOMO-1	-6.667	46	24	11	19
HOMO-2	6.991	13	71	3	13
HOMO-3	-7.261	56	12	13	19
HOMO-4	-7.427	5	91	2	2
HOMO-5	-7.976	36	17	10	37

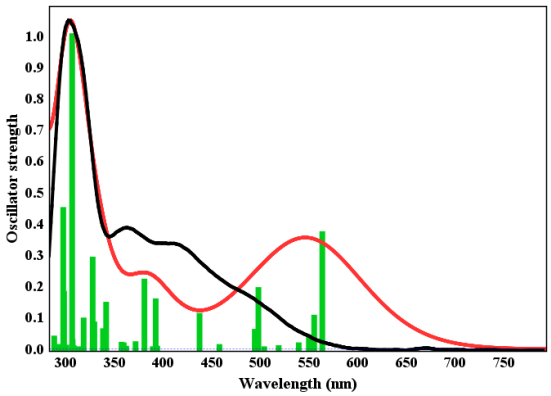

Figure S16. TD-DFT calculated (Red line) and experimental (Black line) UV–vis spectra of **A** in dmso obtained with the mixed basis set 6-31(g)d/LanL2DZ and the functional B3LYP.

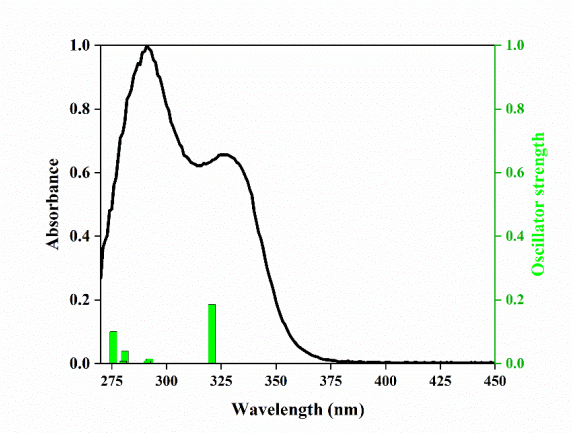

Figure S17. TD-DFT calculated (Green bars) and experimental (Black line) UV–vis spectra of **B** in dmso obtained with the mixed basis set 6-31(g)d/LanL2DZ and the functional B3LYP.

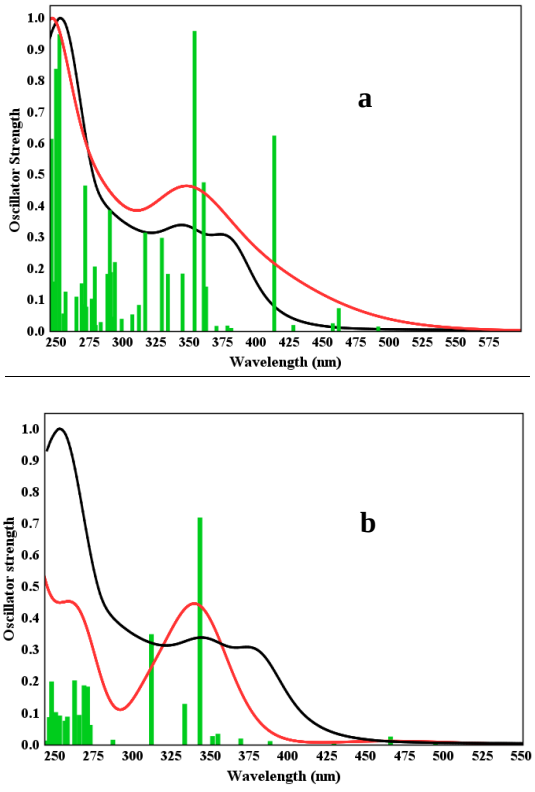

Figure S18. TD-DFT calculated (Red line) and experimental (Black line) UV–vis spectra of **1** in dmso obtained with the mixed basis set 6-31(g)d/LanL2DZ and the functionals B3LYP (a), WB97XD (b).

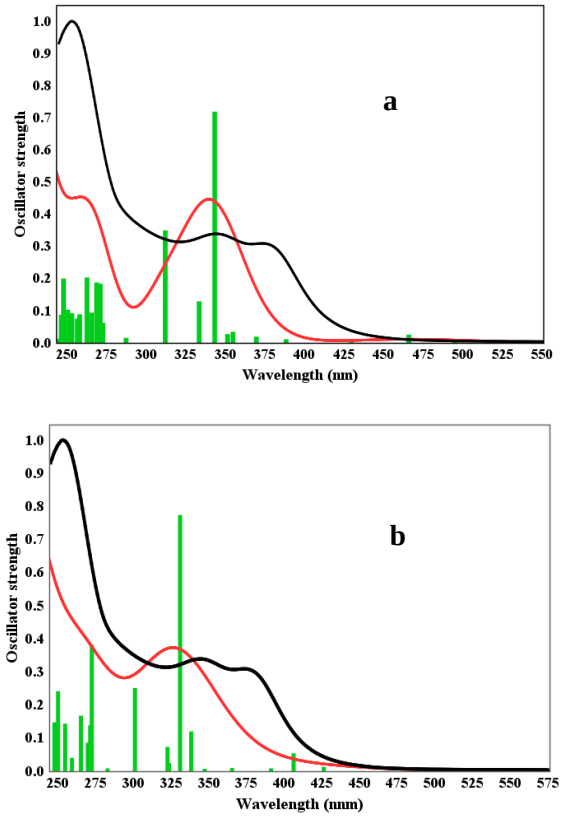

Figure S19. TD-DFT calculated (Red lines) and experimental (Black lines) UV–vis spectra of **1** in dmso obtained with the functional WB97XD and the mixed basis sets 6-31(g)d/LanL2DZ (a), Def2TZVP /LanL2DZ (b).

Table S8. Wavelengths and the nature of transitions for **1** in dmso solution where M = Ru, L_1= bpyNO, L_2 = *p*-cymene and L_3 = Cl.

Exited State	Oscillator Strength	Calculated λ (nm)	Transitions (Percentage Major Contribution)
$S_0 \rightarrow S_1$	0.0009	491.3	HOMO->LUMO (25%), HOMO->L+1 (19%), HOMO->L+2 (40%)
$S_0 \rightarrow S_2$	0.0071	461.7	H-1->L+1 (17%), H-1->L+2 (38%), HOMO->LUMO (11%)
$S_0 \rightarrow S_3$	0.0020	457.2	HOMO->LUMO (60%), HOMO->L+2 (13%)
$S_0 \rightarrow S_5$	0.0655	413.3	H-1->LUMO (75%), H-2->LUMO (3%), H-1->L+2 (8%), HOMO->L+1 (2%)
$S_0 \rightarrow S_{10}$	0.0504	311.2	H-4->LUMO (12%), H-2->LUMO (37%), HOMO->L+1 (18%), HOMO->L+2 (10%)
$S_0 \rightarrow S_{11}$	0.1009	353.5	H-2->LUMO (31%), HOMO->L+1 (36%)
$S_0 \rightarrow S_{14}$	0.0319	278.7	H-1->L+1 (53%), H-1->L+2 (12%), H-1->L+3 (12%), H-2->L+1 (8%), H-2->L+2 (3%), H-1->L+4 (5%)
$S_0 \rightarrow S_{15}$	0.0327	316.5	H-1->L+3 (51%), H-1->L+4 (33%), H-5->LUMO (3%), H-1->L+2 (7%)
$S_0 \rightarrow S_{19}$	0.0227	293.8	H-5->LUMO (25%), H-3->L+1 (25%), H-3->L+2 (9%), H-3->L+3 (2%), H-2->L+1 (4%), H-2->L+2 (5%), HOMO->L+5 (8%)
$S_0 \rightarrow S_{22}$	0.0403	290.0	H-5->LUMO (19%), H-4->L+3 (10%)
$S_0 \rightarrow S_{29}$	0.0486	271.5	H-5->LUMO (25%), H-3->L+1 (25%), H-3->L+2 (9%), H-3->L+3 (2%), H-2->L+1 (4%), H-2->L+2 (5%), HOMO->L+5 (8%)

Table S9. Crystallographic and structure refinement data for **1**.

	1
Empirical formula	$C_{19}H_{22}Cl_2N_4ORu$
Formula weight	494.37
Temperature	100(2) K
Wavelength	0.71073 Å
Crystal system, space group	Monoclinic P21/n
Unit cell dimensions	a = 11.9611(6) Å b = 13.8587(6) Å c = 11.9663(6) Å α= 90° β= 102.052(2)° γ= 90°
Volume	1939.88(16) Å3
Z, Calculated density	1.693 Mg/m3
Absorption coefficient	1.101 mm^{-1}
F(000)	1000
Crystal size	0.022 x 0.220 x 0.272
Theta range for data collection	2.278 to 27.180°
Reflections collected / unique	21686
Absorption correction	semi-empirical from equivalents
Data / restraints / parameters	4305 / 0 / 244
Goodness-of-fit on F^2	1.005
Final R indices [I>2sigma(I)]	R1 = 0.0266, wR2 = = 0.0641
R indices (all data)	R1 = 0.0339 , wR2 = 0.0598

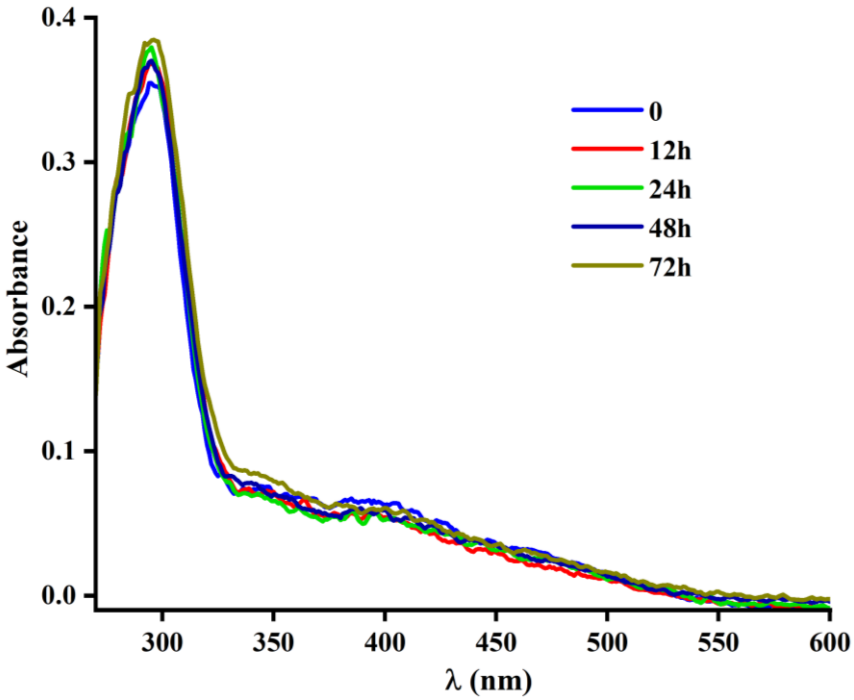

Figure S20. Time course UV-vis spectra of **A** (5×10^{-5} M) dissolved in dmso. The spectra were recorded over 72 hours at room temperature.

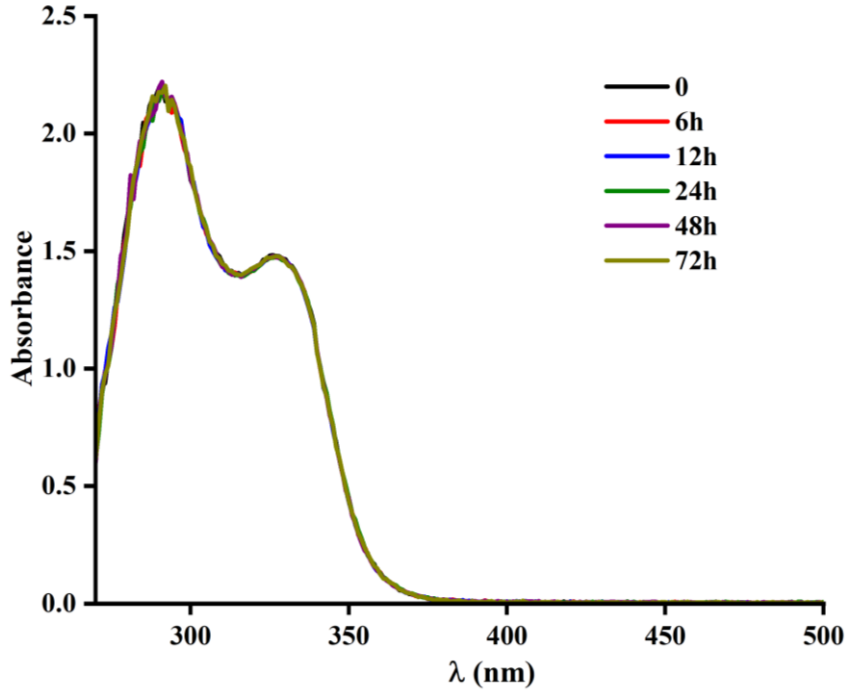

Figure S21. Time course UV-vis spectra of **B** (5×10^{-5} M) dissolved in dmso. The spectra were recorded over 72 hours at room temperature.

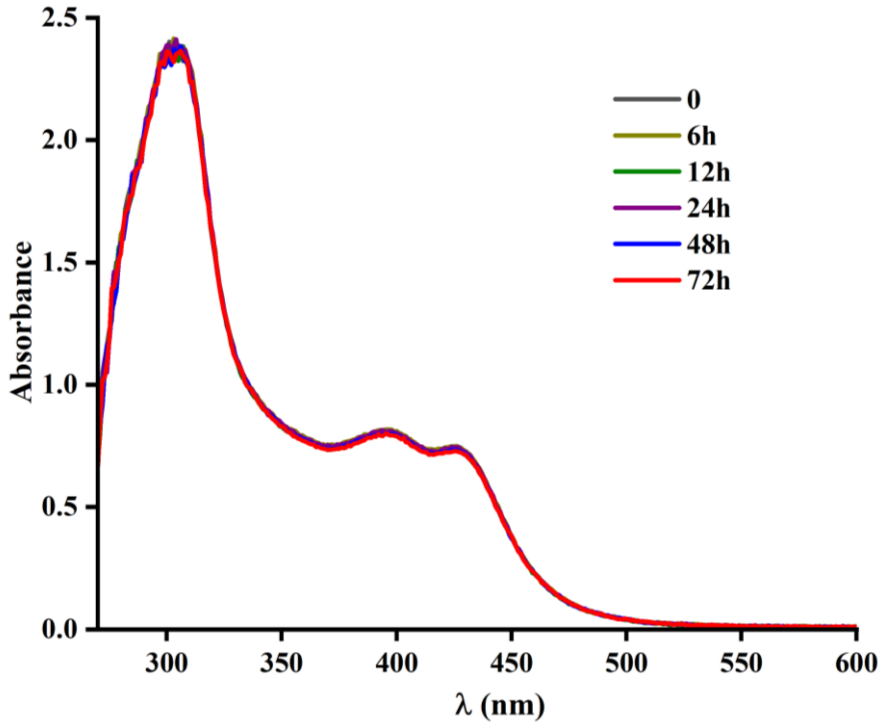

Figure S22. Time course UV-vis spectra of **1** (5×10^{-5} M) dissolved in dmso. The spectra were recorded over 72 hours at room temperature.

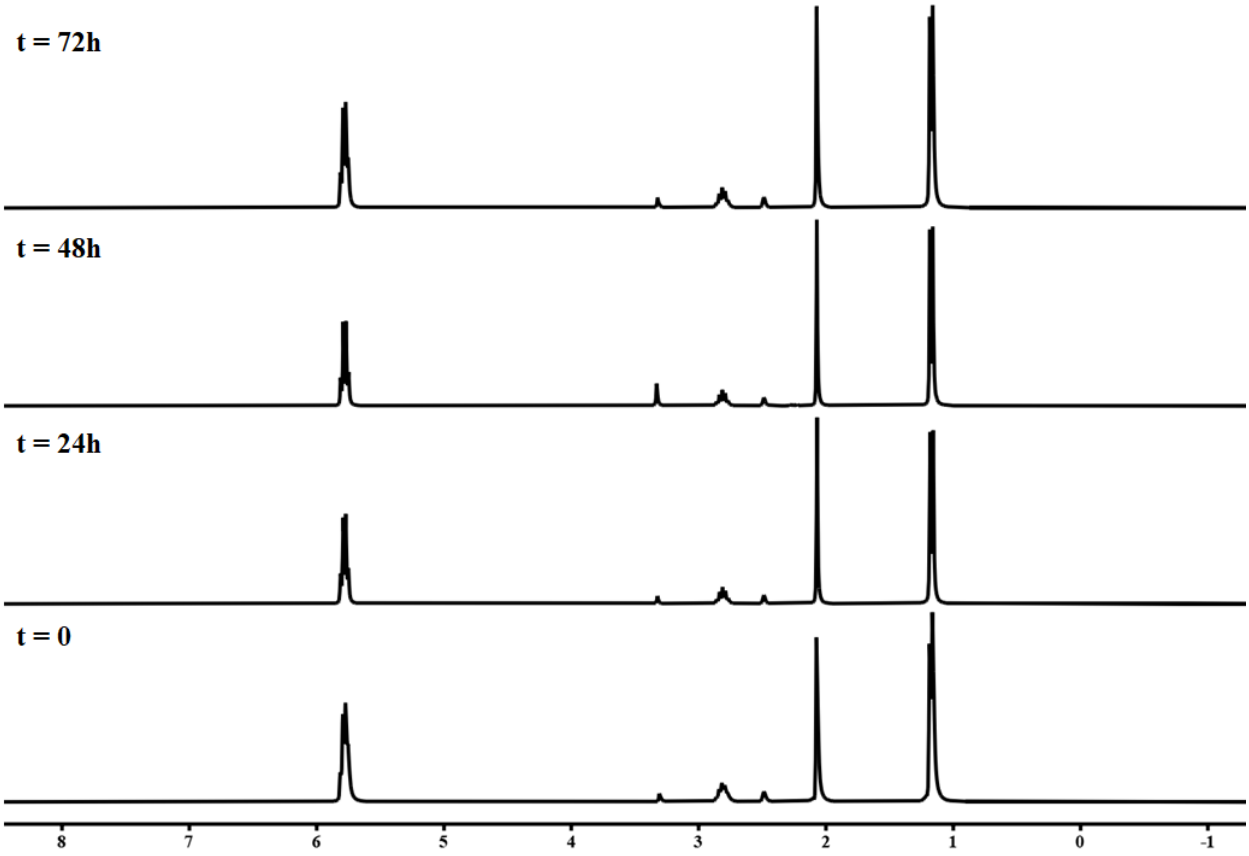

Figure S23. Time course ^{1}H NMR spectrum of **A** in dmso-d_6 at room temperature.

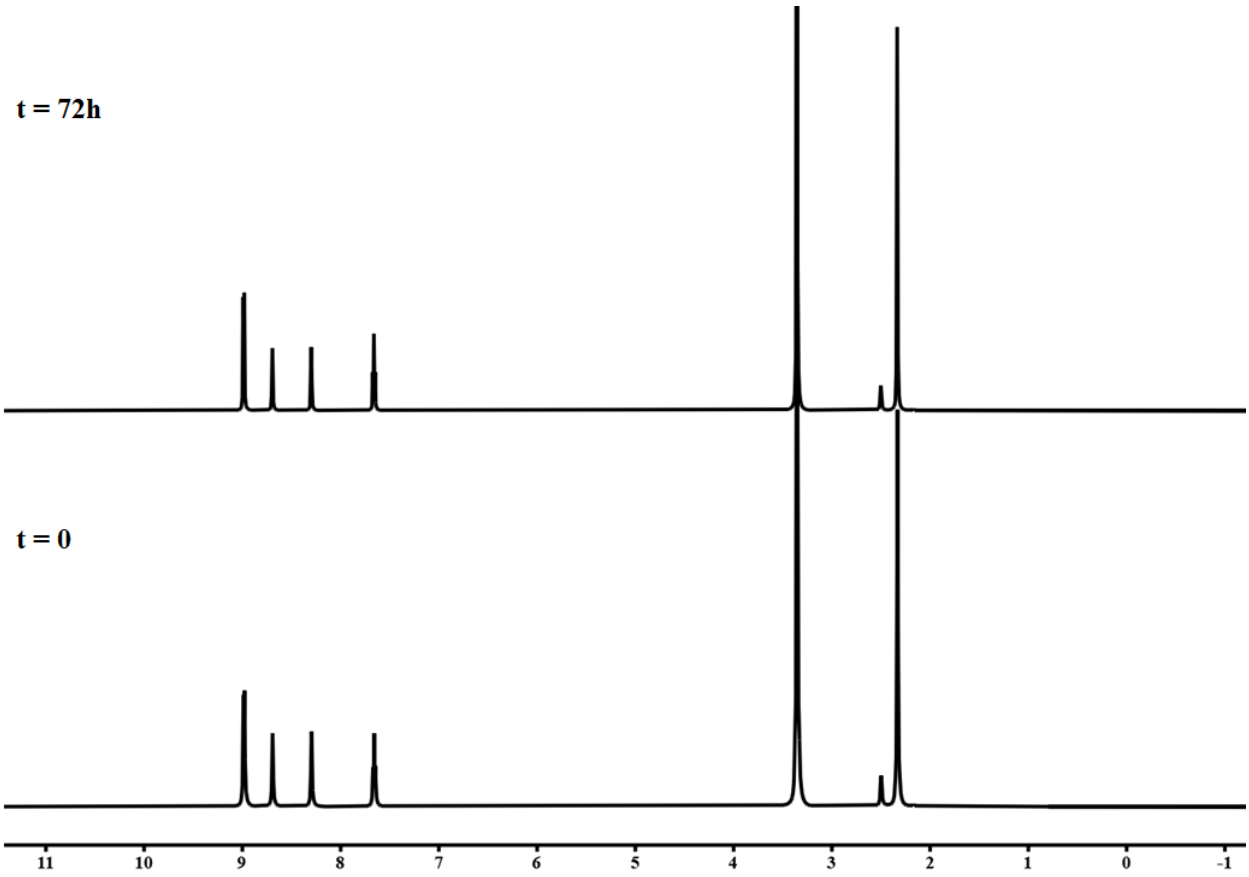

Figure S24. Time course ^{1}H NMR spectrum of **B** in dmso-d_6 at room temperature.

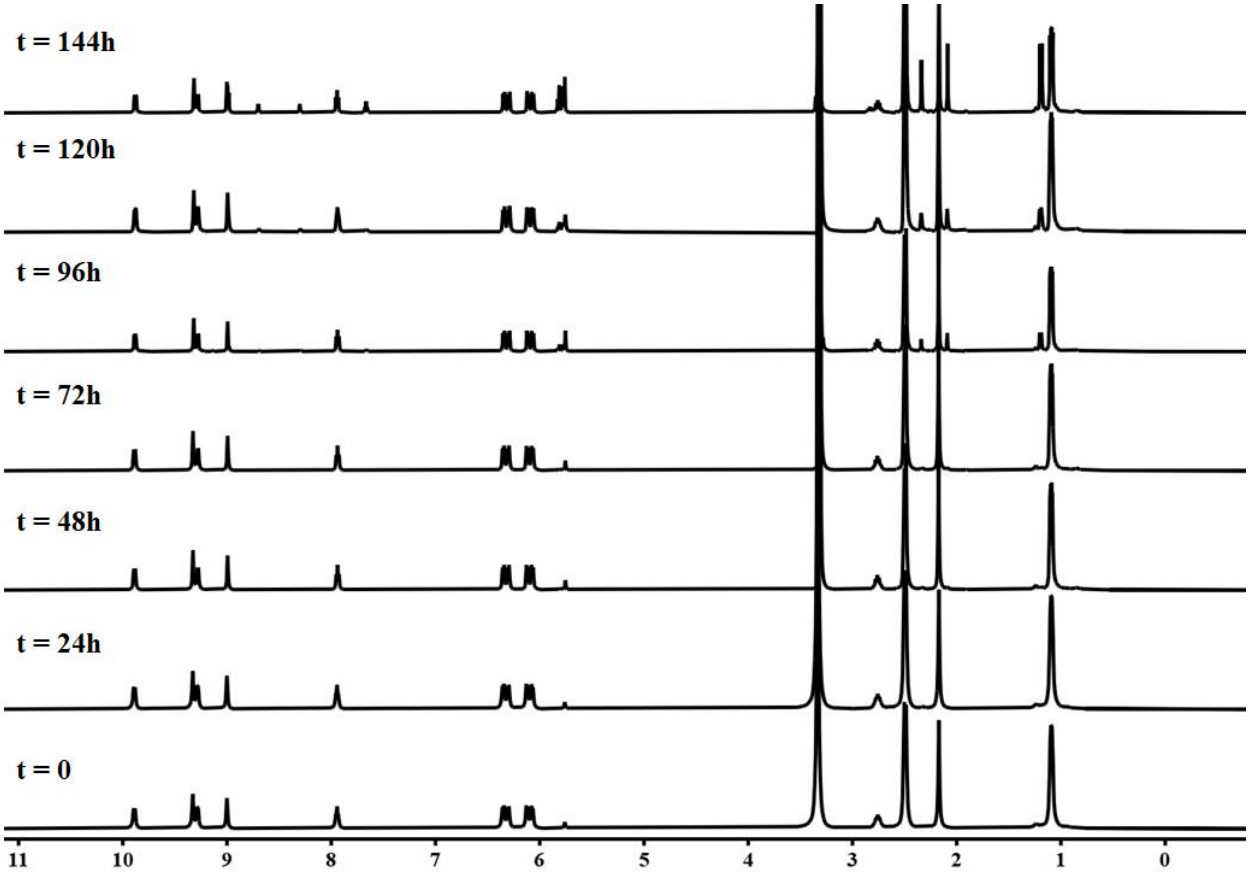

Figure S25. Time course ^{1}H NMR spectrum of **1** in dmso-d_6 at room temperature.

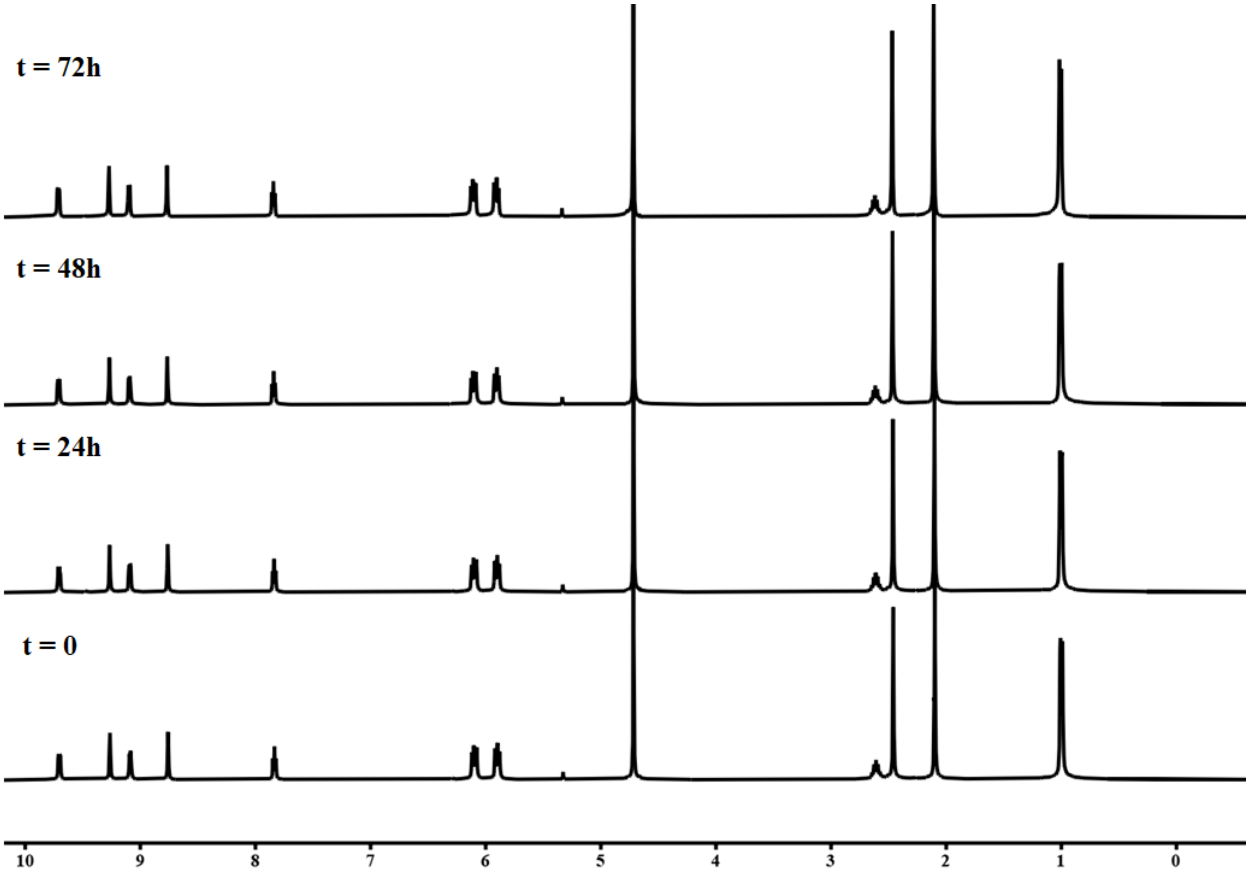

Figure S26. Time course ^{1}H NMR spectrum of **1** in D_2O at room temperature.

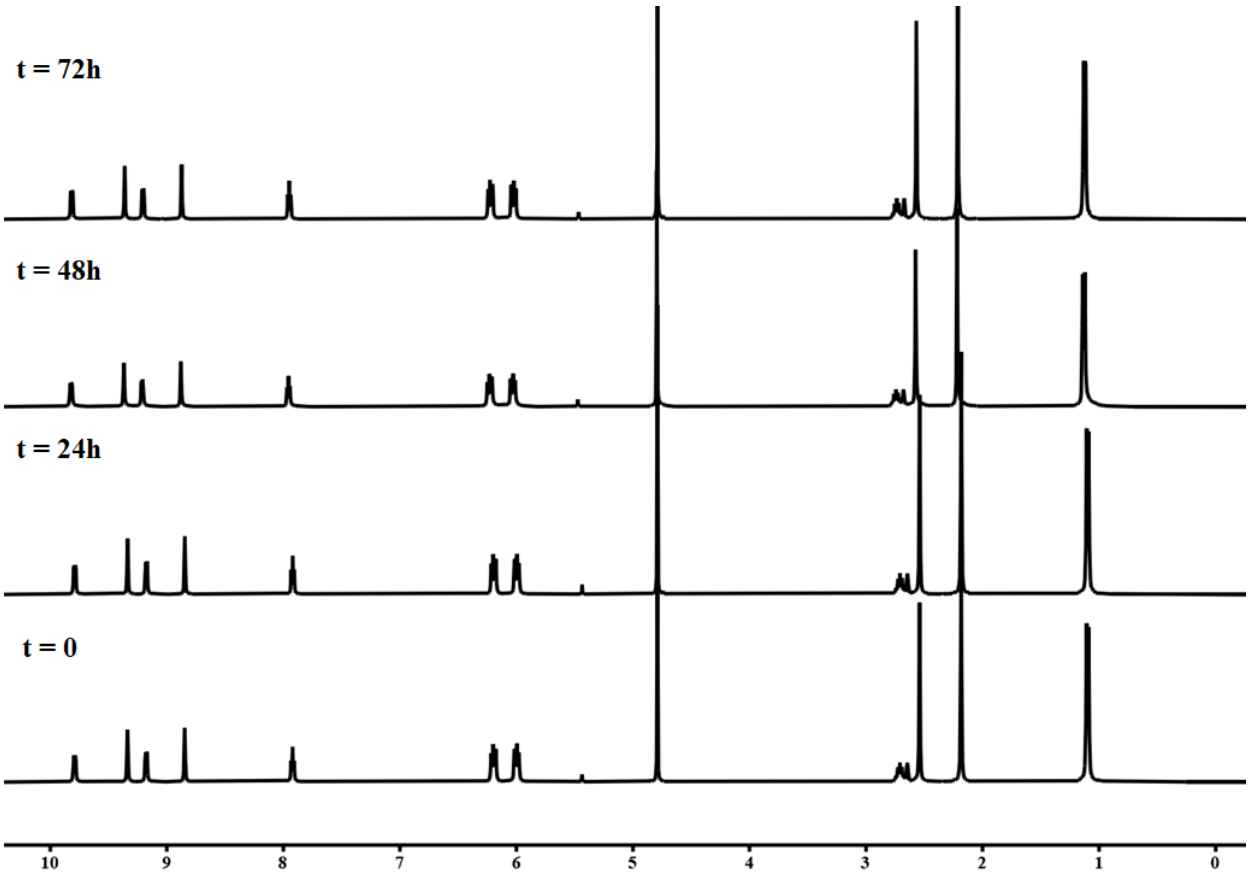

Figure S27. Time course ^{1}H NMR spectrum of **1** in a mixture of dmso-d_6/D_2O at room temperature.

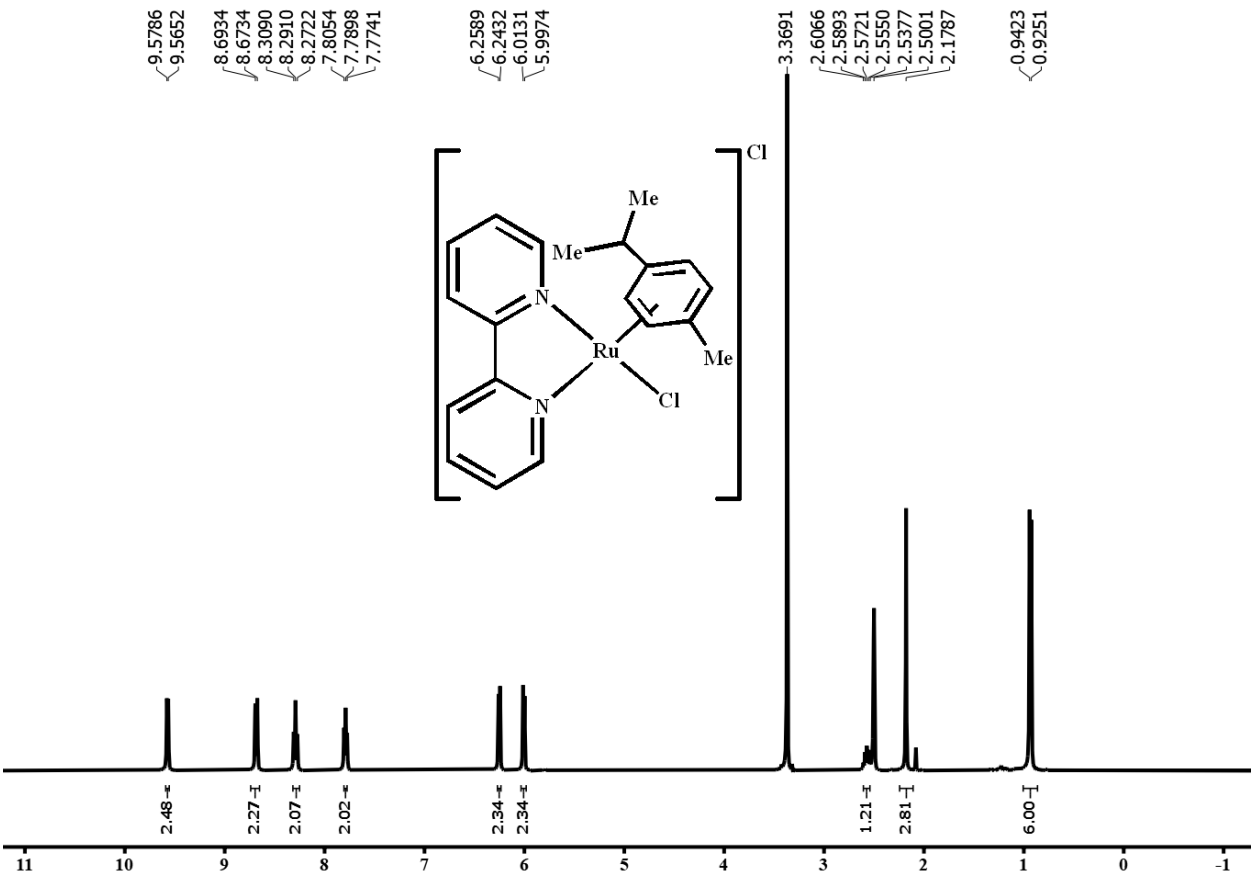

Figure S28. ^{1}H NMR spectrum of **2** in dmso-*d*$_6$.

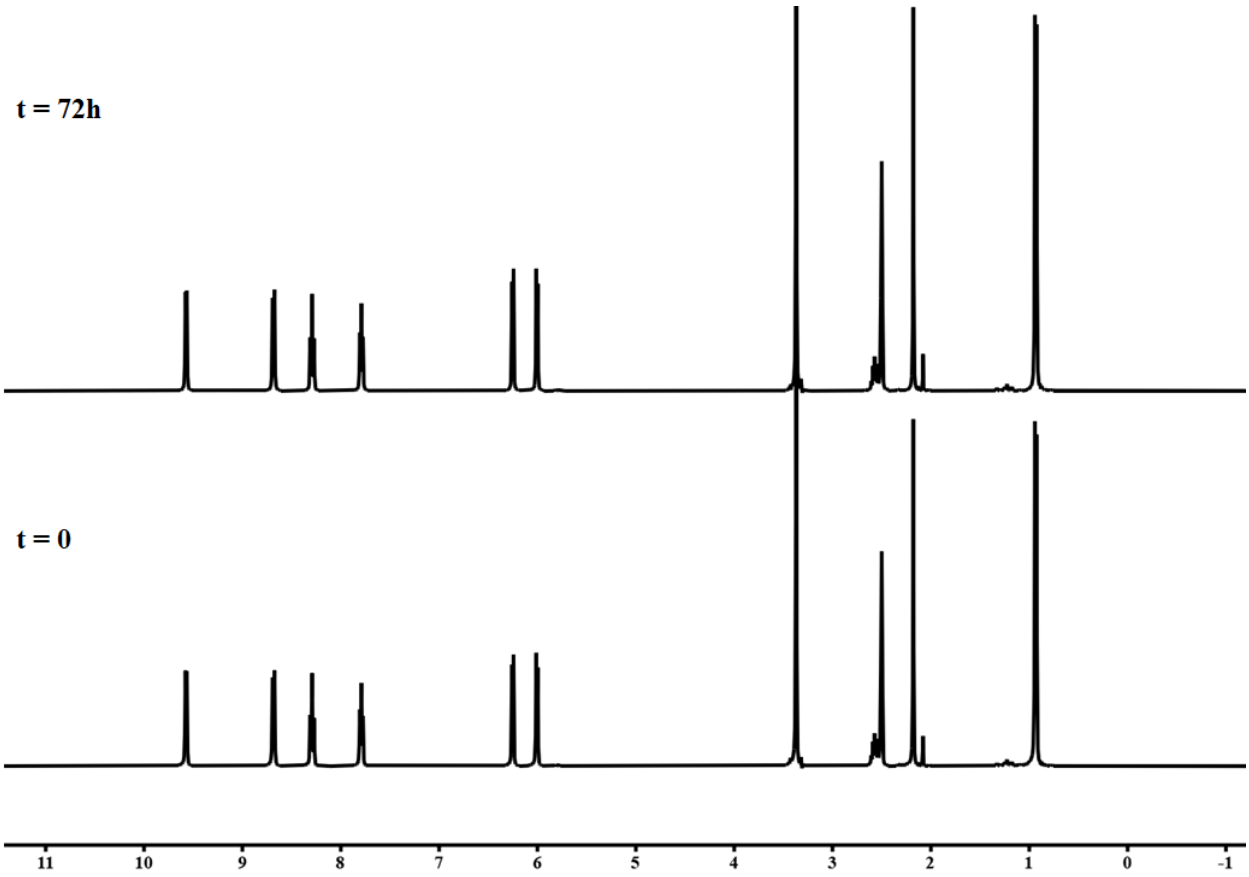

Figure S29. Time course ^{1}H NMR spectrum of **2** in dmso-d_6 at room temperature.

Experimental

General procedures and materials

^{1}H NMR (400 or 300 MHz), and $^{13}C\{^{1}H\}$ (100 MHz) spectra were recorded on a Bruker Avance instrument at 295 K. All chemical shifts (δ) are reported in ppm relative to their corresponding external standards ($SiMe_4$ for ^{1}H and ^{13}C) and the coupling constants (*J*) have being expressed in Hz. The instrument for HR ESI-Mass measurement was a Shimadzu IT-TOF with an electrospray ionization source. Microanalyses were performed with a Thermo Finnigan Flash EA-1112 CHNSO rapid elemental analyzer. UV–vis absorption spectra were carried out using an Ultrospec 4000 Pro or JASCO V-770 UVVisible/NIR. All the reactions were carried out under Argon atmosphere and in the common solvents and all solvents were purified and dried according to standard procedures.[1]

X-ray structure determination

The appropriate crystals of was obtained by slow evaporation of CH_3CN solution of **2** at room temperature. Single crystal X-ray diffraction intensity data of **2** was collected at 100(2) K using a Bruker APEX-II CCD diffractometer equipped with graphite monochromated MoKα radiation (λ = 0.71073 Å). Data reduction was carried out using the program Bruker SAINT[2] and an empirical absorption correction was applied based on multi-scan method.[3] The structure of **2** was solved by direct method and refined by the full-matrix least-square technique on $|F|^2$ with anisotropic thermal parameters to describe the thermal motions of all non-hydrogen atoms using the programs (SHELXS-14)[4] and (SHELXL-18),[5] respectively. All hydrogen atoms were located

from difference Fourier map and refined isotropically. The summary of crystal data and relevant structure refinement parameters for **2** (CCDC 2223210) is given in Table S9.

Computational details

Density functional calculations were performed with the program suite Gaussian 09[6] using the B3LYP level of theory.[7-9] The LanL2DZ basis set was chosen to describe Ru[10, 11] and the 6-31g(d) basis set was chosen for other atoms. The geometries of complexes were fully optimized by employing the density functional theory without imposing any symmetry constraints. In order to ensure the optimized geometries, frequency calculations were performed employing analytical second derivatives. Time-dependent DFT (TD-DFT) calculations were carried out at the same level of theory and basis sets. Solvent effects have been considered by the conductor-like polarizable continuum model (CPCM).[12, 13] The calculations for the electronic absorption spectra by TD-DFT were performed at the same level of theory.

Biological assay

Cell lines and cell culture

Human cancer cell lines, MCF-7 (breast cancer), A549 (non-small cell lung cancer), and Hela (Cervix), were purchased from National Cell Bank of Iran (NCBI, Pasteur Institute, Tehran, Iran). The cells were grown in complete culture media containing RPMI 1640 (Biosera, France), 10% fetal bovine serum (FBS; Gibco, USA) and 1% penicillin−streptomycin (Biosera, France) and kept at 37 °C in a humidified CO_2 incubator. MRC5 cells (human breast epithelial cell line) were cultured in DMEM/Ham's F-12 (GIBCO-Invitrogen, Carlsbad, CA) supplemented with 100 mg/mL cholera toxin, 20 mg/mL epidermal growth factor (EGF), 0.01 mg/mL insulin, 500 mg/mL hydrocortisone, and 5% chelex-treated horse serum.

A standard 3-(4,5-dimethylthiazol-yl)-2,5-diphenyl-tetrazolium bromide (MTT) assay has been used to determine the cytotoxic activities of non-small cell lung cancer, as previously described [14, 15]. To do this, the cells were seeded in 96-well microplates with a density of 0.8×10^4 cells per well and kept for 24h to recover. The cells were then treated in a triplicate manner with compounds (**A**, **1**, and **2**) at varying concentrations ranging from 1 to 100 μM and incubated in a humidified CO_2 incubator for at least 72 hours at 37 °C. The media was completely discarded after incubation and replaced with 150 μL of RPMI 1640 containing 0.5 mg/mL MTT solution and incubated for 3h at room temperature. The media containing MTT was discarded again to dissolve the formazan crystals and 150 μL of dmso was applied to each well and incubated in the dark for at least 30 min at 37 ° C. The absorbance of individual well was then read by ELISA reader at 490 nm. CurveExpert 1.4 was used to measure the 50% inhibitory concentration of each compound, reflecting IC_{50}. The data are is given as mean ± SD.

Apoptosis assay

2×10^5 of MCF-7 cells are pre-cultured for 16 hours followed by exposure to **2** complexes for 24 hours. After mentioned time, AnnexinV/PI staining was performed using eBioscience™ Annexin Vapoptosis detection kit (Invitrogen). Cells were washed once with phosphate buffered saline (PBS), and once with 1000 μL 1X binding buffer. In the next step, the cells were suspended with 100 μL of binding buffer containing 5 μL of Annexin V-fluorescein isothiocyanate for 15 minutes. Afterward, cells were washed again with 1000 μL Binding buffer and resuspended in 200 μL of the same buffer containing 5 μL Propodium Iodide (PI) solution. The apoptosis rates were then determined by BD FACS Calibur™ flow cytometry (BD Biosciences, San Jose, CA, USA). The apoptosis rates were calculated as the sum of early apoptosis and late apoptosis.[16]

Shift mobility assay

Gel electrophoresis analysis was performed using 500 ng plasmid, pBlu2KSM, DNA in 10 mM Tris-HCl buffer, pH 7.4 with the final concentrations of 20–150 µM complex in a total volume of 10 µl. The samples were then incubated for 60 min at 37 °C, followed by electrophoresis on 1% agarose gel in TAE buffer containing 1.0 µg ml^{-1} safe stain at 100 V for 30 min and finally, photographed under UV light. To investigate the DNA-ligand ability of each compound to unwind the supercoiled conformation of pBlu2KSM was determined by electrophoretic mobility on native plasmid. As expected, three different pBlu2KSM conformations were observed on the agarose gels. These were the negative open circular form (NSC) as well as single break nicked supercoil (SSNSC) and a strong bond of the positive twisted supercoiled (PSC). The double strand break of the circular supercoil transform circular DNA to linear (L) format with real length of plasmid is shown as these conformations resolve on agarose gels as distinct bands.

Docking procedure

The two distinct DNA 3D crystal structures (PDB ID: 1BNA, and 1LU5) as well as BSA (PDB ID: 4F5S) have been obtained from the protein data bank (www.rcsb.org/pdb). Co-crystal ligand were extracted from the structures of PDBs. Then, to convert these corrected PDB files to PDBQT, MGLtools 1.5.6 was applied. For the preparation of ligands, the structure of non-small cell lung cancer was sketched using HyperChem Professional (Version 8, Hypercube Inc., Gainesville, FL, USA). Each complex has been optimized using HyperChem 8 by molecular mechanical methods (MM+), followed by measurements of energy minimization at Hartree-Fock (HF) level, using Gaussian 09. Afterwards, the output structures were converted to PDBQT using MGLtools 1.5.6. After the preparation of ligands and receptors, the ligands were docked to DNA using AutoDock 4.2, based on Lamarckian genetic algorithm. By centering the grid box on the minor groove, major groove, and the intercalation site to cover the complete DNA structure, the

grid core on the DNA structures was preserved. The other parameters have all been kept at their default values. In the gpf and dpf data, metal ions parameters (here Ruthenium) for docking were added. With regard to the AutoDock scoring feature, based on the lowest docking binding energy conformation, the best binding mode of ligands and receptors was selected. Docking pose analysis was done using discovery studio visualizer and AutoDock Software 1.5.6.

Cartesian coordinates

A, ground state gas phase

O	0.267300	2.010600	-0.636800
N	0.869800	-1.333500	0.315800
N	0.902200	0.963200	-0.296300
N	-1.821200	0.580300	0.986100
N	-1.878700	-0.904800	-0.892400
C	2.206800	-1.348700	0.338900
H	2.680200	-2.297400	0.580300
C	2.970300	-0.208000	0.067700
C	2.271100	0.944900	-0.255400
H	2.724000	1.894600	-0.512700
C	0.240300	-0.214900	0.025300
C	-1.255000	-0.164200	0.028600
C	-3.156200	0.586800	1.006800
H	-3.625000	1.187100	1.784800
C	-3.920300	-0.133800	0.089200
H	-5.005000	-0.118600	0.112000
C	-3.216500	-0.878600	-0.852900
H	-3.732700	-1.476100	-1.602400
C	4.476500	-0.212000	0.131600
H	4.912500	0.442900	-0.629500
H	4.871600	-1.221100	-0.019400
H	4.828600	0.138600	1.109700

A, ground state dmso solution

O	0.306100	2.038100	-0.660200
N	0.853000	-1.319400	0.311600

N	0.919800	0.971100	-0.301200
N	-1.837000	0.705100	0.882400
N	-1.873900	-1.000900	-0.798100
C	2.188000	-1.353200	0.342500
H	2.648600	-2.307400	0.584600
C	2.971400	-0.221700	0.077200
C	2.287200	0.936400	-0.252500
H	2.758700	1.876500	-0.510300
C	0.237000	-0.187400	0.018600
C	-1.257800	-0.141300	0.021000
C	-3.174800	0.685300	0.913900
H	-3.654500	1.363500	1.616300
C	-3.927500	-0.157300	0.097100
H	-5.011200	-0.162100	0.127300
C	-3.214400	-0.996200	-0.754100
H	-3.723900	-1.687700	-1.421600
C	4.475000	-0.248700	0.150800
H	4.919200	0.544000	-0.457200
H	4.864800	-1.211300	-0.193300
H	4.811400	-0.106600	1.184900

1, ground state, gas phase

Ru	-1.877000	0.078300	0.252900
Ru	1.877100	-0.078100	0.253100
Cl	-1.862000	-2.355900	0.257100
Cl	1.862500	2.356100	0.256800
Cl	0.000100	0.000100	-1.402200
Cl	-0.000100	0.000400	1.908500
C	-2.491000	2.130200	1.027300
C	-3.262400	1.086300	1.654200
H	-3.217200	0.973400	2.732500
C	-3.989000	0.145500	0.891200
H	-4.484800	-0.677200	1.395200
C	-3.974200	0.177000	-0.548800
C	-3.178400	1.180000	-1.156800
H	-3.036700	1.171900	-2.230900
C	-2.457700	2.150900	-0.383200
H	-1.786900	2.837200	-0.888400
C	-1.680400	3.098500	1.843200
H	-2.240500	4.033600	1.977000

H	-0.729100	3.320200	1.350800
H	-1.456300	2.687600	2.830800
C	-4.749100	-0.870800	-1.326600
H	-4.675500	-1.796700	-0.743000
C	-6.234900	-0.458400	-1.401900
H	-6.662900	-0.293500	-0.406400
H	-6.818900	-1.244400	-1.893600
H	-6.358600	0.465700	-1.979800
C	-4.177600	-1.164200	-2.719800
H	-4.278700	-0.306000	-3.396000
H	-4.727000	-1.997000	-3.171400
H	-3.122400	-1.447000	-2.658700
C	2.490800	-2.129800	1.028200
C	2.457300	-2.151000	-0.382300
H	1.786300	-2.837400	-0.887200
C	3.178000	-1.180500	-1.156400
H	3.036000	-1.172700	-2.230500
C	3.974100	-0.177400	-0.548900
C	3.989200	-0.145400	0.891000
H	4.485200	0.677400	1.394600
C	3.262600	-1.085800	1.654600
H	3.217700	-0.972600	2.732800
C	1.680300	-3.097800	1.844600
H	0.729100	-3.319900	1.352200
H	1.456000	-2.686200	2.831900
H	2.240600	-4.032600	1.979100
C	4.748900	0.870000	-1.327200
H	4.675500	1.796100	-0.744000
C	4.177400	1.162800	-2.720500
H	4.278300	0.304400	-3.396400
H	4.726800	1.995500	-3.172500
H	3.122200	1.445800	-2.659500
C	6.234700	0.457500	-1.402500
H	6.358300	-0.466900	-1.980000
H	6.662800	0.292900	-0.407000
H	6.818700	1.243200	-1.894600

1, ground state, dmso solution

Ru	1.923200	0.053800	-0.258200
Ru	-1.923200	-0.053700	-0.258300

Cl	1.860300	-2.414300	-0.268300
Cl	-1.860600	2.414400	-0.267900
Cl	-0.000100	-0.000000	1.385200
Cl	0.000000	0.000300	-1.902000
C	2.657300	2.057900	-1.097500
C	3.390200	0.956900	-1.664500
H	3.383400	0.810200	-2.739100
C	4.061400	0.026700	-0.843000
H	4.551600	-0.824700	-1.302200
C	4.024200	0.124400	0.591400
C	3.244900	1.172400	1.139100
H	3.092400	1.225900	2.210200
C	2.584100	2.135600	0.309400
H	1.960600	2.892200	0.772300
C	1.958600	3.049200	-1.982200
H	2.676800	3.816500	-2.298300
H	1.137400	3.542200	-1.456500
H	1.563400	2.567300	-2.880200
C	4.781000	-0.888600	1.429500
H	4.679900	-1.852600	0.916200
C	6.278800	-0.509500	1.440100
H	6.686300	-0.439700	0.425700
H	6.849200	-1.270800	1.982900
H	6.435100	0.454300	1.938600
C	4.244000	-1.054400	2.856900
H	4.397900	-0.151300	3.459100
H	4.778400	-1.870900	3.353200
H	3.176200	-1.297000	2.860600
C	-2.657300	-2.057500	-1.098300
C	-2.583900	-2.135800	0.308600
H	-1.960300	-2.892500	0.771100
C	-3.244600	-1.172900	1.138700
H	-3.092000	-1.226900	2.209800
C	-4.024100	-0.124800	0.591600
C	-4.061400	-0.026500	-0.842800
H	-4.551800	0.825100	-1.301600
C	-3.390300	-0.956300	-1.664800
H	-3.383700	-0.809200	-2.739400
C	-1.958600	-3.048400	-1.983500
H	-1.137300	-3.541500	-1.458100

H	-1.563600	-2.566000	-2.881400
H	-2.676800	-3.815600	-2.299800
C	-4.780900	0.887900	1.430200
H	-4.679700	1.852100	0.917300
C	-4.243800	1.052900	2.857600
H	-4.397900	0.149500	3.459400
H	-4.778200	1.869200	3.354300
H	-3.176000	1.295500	2.861500
C	-6.278700	0.508800	1.440500
H	-6.435000	-0.455200	1.938600
H	-6.686200	0.439700	0.426100
H	-6.849000	1.269900	1.983800

2, ground state, gas phase

Ru	0.70451500	-0.37162800	-0.42220200
Cl	-0.18149100	-0.94917300	-2.59128300
O	-4.14603700	1.32570700	0.73904200
N	-1.27361100	-0.68447900	0.25467600
N	-3.38622300	0.33012700	0.67333900
N	-2.23109200	2.71270700	-0.56227300
N	-0.20981800	1.47157800	-0.77478800
C	-1.73743000	-1.87141800	0.64251300
H	-1.04733200	-2.70386600	0.60683800
C	-3.07244100	-2.03490900	1.05485000
C	-3.86259600	-0.90926500	1.06605100
H	-4.89976400	-0.87823600	1.37496300
C	-2.07293600	0.40312900	0.22235000
C	-1.50909400	1.61383200	-0.37797700
C	-1.65705900	3.73371600	-1.20188400
H	-2.27103400	4.62055400	-1.33831400
C	-0.34965500	3.67028300	-1.68327900
H	0.10744800	4.49057300	-2.22452000
C	0.34673000	2.49210500	-1.44731300
H	1.35797600	2.34121400	-1.80404000
C	-3.60854900	-3.38198300	1.45990600
H	-3.61463400	-4.06507800	0.60260700
H	-4.63000200	-3.30674400	1.83998300
H	-2.98577400	-3.83457900	2.23926800
C	2.33335200	0.29915500	1.10457600
C	2.84761200	0.36099600	-0.23799400

H	3.22014400	1.30996600	-0.61286500
C	2.83991600	-0.75343700	-1.09290700
H	3.17736200	-0.64925600	-2.11832300
C	2.34957200	-2.03179700	-0.64156000
C	1.81755000	-2.08981100	0.65736000
H	1.39230300	-3.02249700	1.01431800
C	1.78565500	-0.93647900	1.51079800
H	1.32450200	-1.02552300	2.48790300
C	2.42228700	1.52049300	2.00335100
H	2.28660300	2.39896800	1.35723500
C	1.35169800	1.57413400	3.10182200
H	1.49151700	0.78340200	3.84793000
H	0.33965700	1.48724000	2.69058300
H	1.41720200	2.52862100	3.63268200
C	3.84315300	1.60140600	2.60704200
H	4.03696300	0.74779600	3.26637000
H	3.94555900	2.51660600	3.19893600
H	4.61651500	1.61313000	1.83141200
C	2.36208400	-3.21585300	-1.56419900
H	1.84356400	-2.97377100	-2.49787500
H	1.87589200	-4.08317700	-1.11054700
H	3.39640900	-3.48875300	-1.80591100

2, ground state, dmso solution

Ru	0.70451500	-0.37162800	-0.42220200
Cl	-0.18149000	-0.94917300	-2.59128300
O	-4.14603700	1.32570700	0.73904200
N	-1.27361100	-0.68447900	0.25467600
N	-3.38622300	0.33012700	0.67333900
N	-2.23109200	2.71270700	-0.56227300
N	-0.20981700	1.47157800	-0.77478900
C	-1.73743000	-1.87141800	0.64251300
H	-1.04733200	-2.70386600	0.60683800
C	-3.07244100	-2.03490900	1.05485000
C	-3.86259600	-0.90926500	1.06605100
H	-4.89976400	-0.87823500	1.37496300
C	-2.07293600	0.40312900	0.22235000
C	-1.50909400	1.61383200	-0.37797700
C	-1.65705900	3.73371600	-1.20188400
H	-2.27103400	4.62055400	-1.33831400

C	-0.34965500	3.67028300	-1.68328000
H	0.10744800	4.49057200	-2.22452000
C	0.34673000	2.49210500	-1.44731300
H	1.35797600	2.34121400	-1.80404000
C	-3.60854900	-3.38198300	1.45990600
H	-3.61463400	-4.06507800	0.60260700
H	-4.63000200	-3.30674300	1.83998300
H	-2.98577400	-3.83457900	2.23926800
C	2.33335200	0.29915500	1.10457600
C	2.84761100	0.36099600	-0.23799400
H	3.22014400	1.30996600	-0.61286500
C	2.83991600	-0.75343700	-1.09290600
H	3.17736300	-0.64925600	-2.11832300
C	2.34957300	-2.03179700	-0.64155900
C	1.81755000	-2.08981100	0.65736100
H	1.39230300	-3.02249700	1.01431900
C	1.78565500	-0.93647900	1.51079800
H	1.32450100	-1.02552200	2.48790300
C	2.42228700	1.52049300	2.00335100
H	2.28660200	2.39896800	1.35723500
C	1.35169800	1.57413300	3.10182300
H	1.49151700	0.78340200	3.84793000
H	0.33965700	1.48724000	2.69058300
H	1.41720200	2.52862000	3.63268200
C	3.84315300	1.60140700	2.60704200
H	4.03696300	0.74779600	3.26637000
H	3.94555900	2.51660600	3.19893600
H	4.61651500	1.61313100	1.83141200
C	2.36208400	-3.21585300	-1.56419900
H	1.84356400	-2.97377100	-2.49787500
H	1.87589200	-4.08317700	-1.11054700
H	3.39640900	-3.48875300	-1.80591000

References

1. Armarego, W. L., *Purification of laboratory chemicals*. Butterworth-Heinemann2017.

2. Bruker *SAINT*, Version 6.36 a. *Bruker-AXS Inc.: Madison, WI, USA* **2002**.

3. Bruker *SMART*, Version 5.625 and SADABS, version 2.03 a. *Bruker AXS Inc., Madison, Wisconsin* **2001**.

4. Sheldrick, G. M., A short history of *SHELX*. *Acta Cryst.* **2008**, *A64*, 112-122.

5. Sheldrick, G. M., Crystal structure refinement with *SHELXL*. *Acta Cryst.* **2015**, *C27*, 3-8.

6. Frisch, M. J.; Trucks, G. W.; Schlegel, H. B.; Scuseria, G. E.; Robb, M. A.; Cheeseman, J. R.; Scalmani, G.; Barone, V.; Mennucci, B.; Petersson, G. A.; Nakatsuji, H.; Caricato, M.; Li, X.; Hratchian, H. P.; Izmaylov, A. F.; Bloino, J.; Zheng, G.; Sonnenberg, J. L.; Hada, M.; Ehara, M.; Toyota, K.; Fukuda, R.; Hasegawa, J.; Ishida, M.; Nakajima, T.; Honda, Y.; Kitao, O.; Nakai, H.; Vreven, T.; Montgomery, J. J. A.; Peralta, J. E.; Ogliaro, F.; Bearpark, M.; Heyd, J. J.; Brothers, E.; Kudin, K. N.; Staroverov, V. N.; Keith, T.; Kobayashi, R.; Normand, J.; Raghavachari, K.; Rendell, A.; Burant, J. C.; Iyengar, S. S.; Tomasi, J.; Cossi, M.; Rega, N.; Millam, J. M.; Klene, M.; Knox, J. E.; Cross, J. B.; Bakken, V.; Adamo, C.; Jaramillo, J.; Gomperts, R.; Stratmann, R. E.; Yazyev, O.; Austin, A. J.; Cammi, R.; Pomelli, C.; Ochterski, J. W.; Martin, R. L.; Morokuma, K.; Zakrzewski, V. G.; Voth, G. A.; Salvador, P.; Dannenberg, J. J.; Dapprich, S.; Daniels, A. D.; Farkas, O.; Foresman, J. B.; Ortiz, J. V.; Cioslowski, J.; Fox, D. J., *Gaussian 09, Revision A.02*. 2016; p Gaussian, Inc., Wallingford CT.

7. Becke, A. D., Density-functional Thermochemistry. III. The Role of Exact Exchange. *J. Chem. Phys.* **1993**, *98*, 5648-5652.

8. Miehlich, B.; Savin, A.; Stoll, H.; Preuss, H., Results Obtained with the Correlation Energy Density Functionals of Becke and Lee, Yang and Parr. *Chem. Phys. Lett.* **1989**, *157*, 200-206.

9. Lee, C.; Yang, W.; Parr, R. G., Development of the Colle-Salvetti Correlation-Energy Formula into a Functional of the Electron Density. *Phys. Rev. B* **1988**, *37*, 785.

10. Wadt, W. R.; Hay, P. J., Ab Initio Effective Core Potentials for Molecular Calculations. Potentials for Main Group Elements Na to Bi. *J. Chem. Phys.* **1985**, *82*, 284-298.

11. Roy, L. E.; Hay, P. J.; Martin, R. L., Revised Basis Sets for the LANL Effective Core Potentials. *J. Chem. Theory Comput.* **2008**, *4*, 1029-1031.

12. Cossi, M.; Scalmani, G.; Rega, N.; Barone, V., New Developments in the Polarizable Continuum Model for Quantum Mechanical and Classical Calculations on Molecules in Solution. *J. Chem. Phys.* **2002**, *117*, 43-54.

13. Barone, V.; Cossi, M.; Tomasi, J., A New Definition of Cavities for the Computation of Solvation Free Energies by the Polarizable Continuum Model. *J. Chem. Phys.* **1997**, *107*, 3210-3221.

14. Fereidoonnezhad, M.; Shahsavari, H. R.; Abedanzadeh, S.; Nezafati, A.; Khazali, A.; Mastrorilli, P.; Babaghasabha, M.; Webb, J.; Faghih, Z.; Faghih, Z.; Beyzavi, M. H., Synthesis, structural characterization, biological evaluation and molecular docking studies of new platinum(II) complexes containing isocyanides. *New J. Chem.* **2018**, *42*, 8681-8692.

15. Fereidoonnezhad, M.; Shahsavari, H. R.; Abedanzadeh, S.; Behchenari, B.; Hossein-Abadi, M.; Faghih, Z.; Beyzavi, M. H., Cycloplatinated(II) complexes bearing 1,1′-

bis(diphenylphosphino)ferrocene ligand: biological evaluation and molecular docking studies. *New J. Chem.* **2018**, *42*, 2385-2392.

16. Fereidoonnezhad, M.; Kaboudin, B.; Mirzaee, T.; Babadi Aghakhanpour, R.; Golbon Haghighi, M.; Faghih, Z.; Faghih, Z.; Ahmadipour, Z.; Notash, B.; Shahsavari, H. R., Cyclometalated Platinum(II) Complexes Bearing Bidentate O, O′-Di(alkyl)dithiophosphate Ligands: Photoluminescence and Cytotoxic Properties. *Organometallics* **2017**, *36*, 1707-1717.